1974

Interaction forces between ships.

Fortson, Robert Malcolm.

Massachusetts Institute of Technology

INTERACTION FORCES BETWEEN SHIPS

Robert Malcolm Fortson

INTERACTION FORCES BETWEEN SHIPS

by

ROBERT MALCOLM FORTSON, III

B. S. United States Naval Academy

(1969)

SUBMITTED IN PARTIAL FULFILLMENT

OF THE REQUIREMENTS FOR THE

DEGREE OF OCEAN ENGINEER

at the

MASSACHUSETTS INSTITUTE OF TECHNOLOGY

May 10, 1974

INTERACTION FORCES BETWEEN SHIPS

by

ROBERT M. FORTSON, III

Submitted to the Department of Ocean Engineering on May 10, 1974, in partial fulfillment of the requirements for the degree of Ocean Engineer.

ABSTRACT

The thesis develops a theoretical model for predicting ship interactions that should be useful in a ship trajectory analysis. The method assumes that when ships are close together, the potential field is the main source of the interaction forces. The flows around the ships are represented by using half bodies of revolution generated with axial singularity distributions. A second axial distribution of doublets were included to correct for cross flows and thus maintain the rigid body boundary condition. Following the determination of the fluid flows, the forces were calculated using Lagally's theorem as expanded by W. E. Cummins.

The principal result was a computerized model to predict forces resulting from steady, parallel motion of bodies of revolution moving in an infinite ideal fluid. The program is capable of handling ship geometries in rectilinear motion. It was found that the theoretical model produced similar results when compared with model tests conducted by D. W. Taylor, however, those tests were reported as being crude. This emphasizes the need to obtain a set of more valid empirical data.

Thesis Supervisor: Martin A. Abkowitz
Title: Professor of Ocean Engineering

ACKNOWLEDGEMENTS

My thanks goes first to Martin A. Abkowitz for suggesting the topic of this thesis and having patience during the many revisions of the computer program.

Also, I dedicate this work to my wife, Martha, who spent many hours with the editing and typing especially on Mother's Day.

TABLE OF CONTENTS

LIST OF FIGURES

LIST OF TABLES

CHAPTER I

INTRODUCTION

1.1 General

Interactions between ships operating in proximity can be thought of as a modern day phenomena. There are no known references to it in the literature until after the emergence of steam driven ships. Along with the increase in shipping in shallow and restricted waters, this innovation contributed to the higher frequency of collisions. These collisions provided the operator with his initial encounters with ship interaction forces. It was many years, however, before the courts recognized the existence of this strange force which contributed to many of the collisions. The acceptance of these forces came only after many eyewitness accounts described strange ship behaviors and it was concluded that there must have been a force that was not present during normal operations.

With the increased density of shipping in restricted waters, especially for channels, it is not surprising that collisions involving interactions were first noticed for the shallow water occurrences. The effect of shallow water has persisted as being important in describing the interaction phenomena. Shallow water does influence the flow around the ship, however, for depths greater than twice the draft of the ship, the effect of the ocean bottom is

expected to be small. This is based upon the interaction between ships in deep water, forces have been experimentally determined as the ship separation was increased.

With the increased speeds and maneuverability introduced by steam propulsion, interactions other than with ships were first noticed and recorded. These involved the forces experienced by the position of the ship in the channel. From these forces, rules of thumb were formed such as the ship "smells the bank". This particular rule indicates the mariner realized that the ship interacts with the channel bank so as to sheer away from it. It is in this area of ship maneuverability in restricted water that a great many empirical studies have been made. With the results of Bernoulli, the mechanism could be explained. Even today the operators aware of the Venturi effect tend to associated all interactions and explain them consistent with this law. This may give a rough guide, but does not contribute to the understanding of the process. It may at times even lead an investigator to the wrong conclusions.

The forces evolving from ship interactions has long been a controversial subject. The main interest has stemmed from the cases which result from collisions. The literature is sprinkled with accounts of major collisions. Included are discussions where important figures of the day give conflicting explanations of the ships' behavior. The first

scientific investigations involving model tests occurred in 1909 when D. W. Taylor presented his findings to the Society of Naval Architects and Marine Engineers. The discussions of the paper demonstrated the debate at the time about the causes of the forces.

The study of interaction forces is important for at least four reasons. First, they contribute to collisions. The understanding of these forces is necessary to help prevent future occurrences. Second is for the control of ships moving in proximity to each other, as done by several Navys to accomplish refueling of ships at sea. The third implication is in the design of future ships and their operating procedures. The adverse effects of ship interactions may be reduced by modifying design parameters and effective design and use of controls. Finally, for those ships in operation, the present rules for navigation do not recognize the interaction effects. Future study may show the need to modify these rules so as to provide safer movement of the merchant fleet.

With this perspective, the research effort here attempts to determine the extent of the past efforts to develop a generalized theory for ship interactions which would be practical to the engineer. The view is toward a general model, in particular one which could be used as part of a generalized program for predicting ship trajectories.

1.2 Ship Interaction

1.2.1 General

What is meant by interaction forces? Any force that is only observed when one or more ships (or other objects such as wall, etc.) are present can be classified as an interaction force. The motion of a ship through the water manifests itself by waves and the wake formed and by a moving pressure disturbance in the water. The moving pressure field will be identified as the potential disturbance where the waves will be referred to as the free surface disturbance.

The interactions between ships operating on the surface of the ocean result from the influence of both the free surface and potential disturbances, whereas each appears to create forces by different mechanisms and differ in their spatial distribution. The potential field generates a distribution of pressures in the fluid. The waves also generate a pressure field. However, this rapidly attenuates with depth. The waves also change the water surface and this introduces forces. If the frequency is low, the long duration of the force will cause significant ship motions. An example is in the case of following seas where directional instability may occur and result in a large response of the ship.

Very close to the ship, the potential field dominates

the fluid flow pattern, where much further away the waves produce the flow disturbances. The induced flows act on other bodies (ships) placed in the perturbed stream to create interaction forces.

1.2.1 Taylor Results

One of the first scientific experiments performed and reported on the interaction between ships was conducted by David W. Taylor at the Model Basin in Washington, D. C. The results are reported in the 1909 Transaction of Society of Naval Architects and Marine Engineers. A good summary of the work can be found in Reference 2. Here attention is focused on the quantitative measurements. The results are presented for the two model trials. The first is with relatively thin models and the second is with fuller models. For convenience, the model characteristics are also presented. In each case, the forces are reported for only one of the models as indicated.

MODEL	LENGTH	BEAM	DRAFT	
834*	20.512	3.69	1.26	THIN
838	20.512	3.50	1.20	
858*	20.512	3.59	.96	FULL
866	20.512	2.78	1.24	

* FORCES DETERMINED

TABLE I

FIGURE I

TAYLOR'S RESULTS

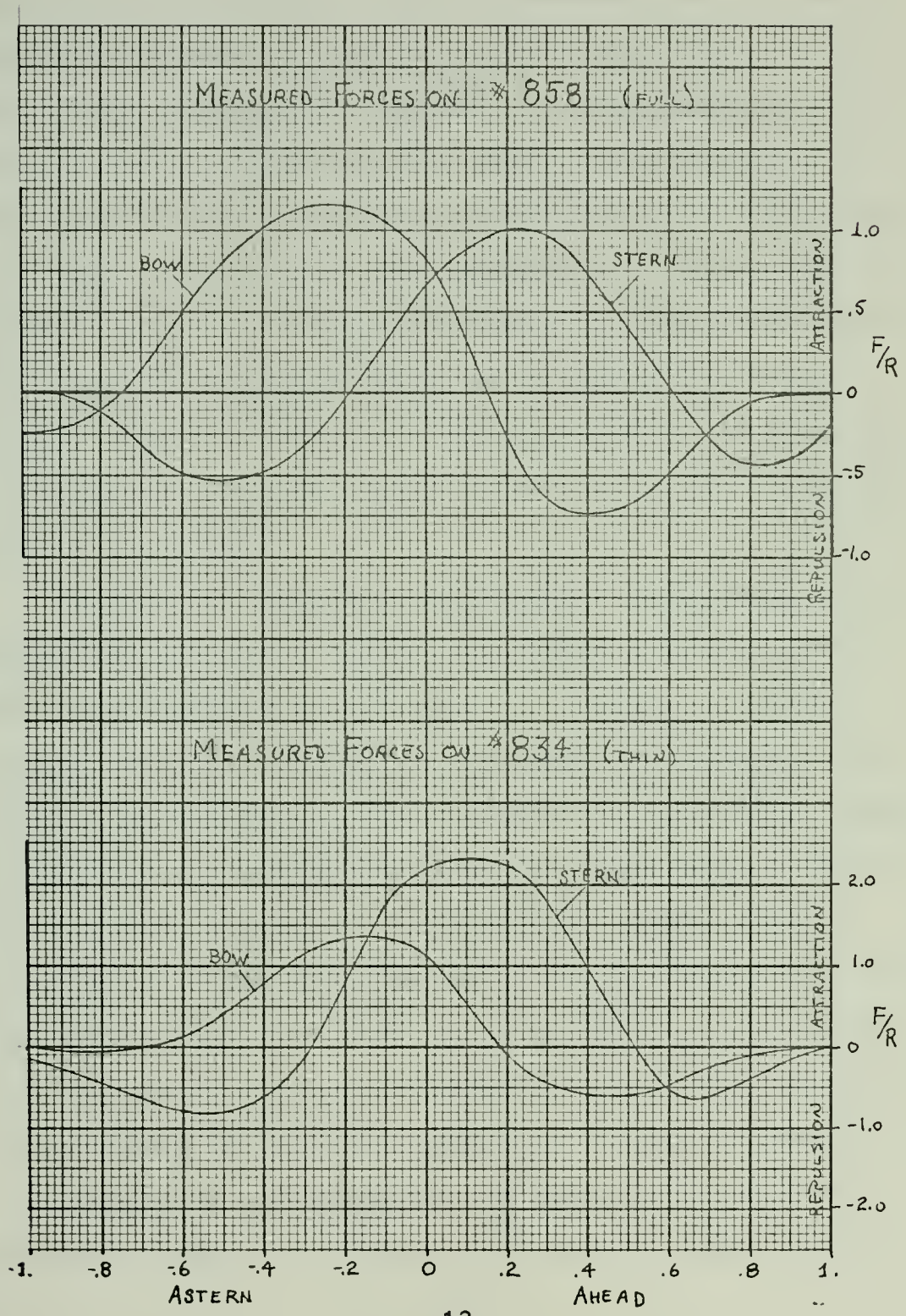

The original results were non-dimensionalized by the resistance of the model. Taylor comments that the results may have inaccuracies due to problems encountered in towing the models on a parallel course. He also stated that the results for the thinner models were less consistant. It is difficult to say if the data was erratic or if the results were counter intuitive, thus indicating to Taylor that they might be erratic. Whatever the meaning, both results are presented and evaluated using the proposed theoretical models. Appendix E contains calculations of the possible errors in the data that might have resulted from misalignment in the models.

The original data was modified to develop the total forces and moments on the models. Also a change in the non-dimensionalization was made. To accomplish these changes, the force acting on the model was determined by multiplying the data by the resistance of the model. Taylor states that the models were towed at speed between two and three knots. A value of 2.5 knots was assumed. The total force on the model is determined by adding the forces that were measured at each end of the model. The moments were calculated about the midship position. The following curves depict Taylor's data after the indicated changes.

The curves are drawn for the ships in various relative positions. The abscissa is scaled in terms of the

FIGURE 2

TAYLOR MODEL TESTS

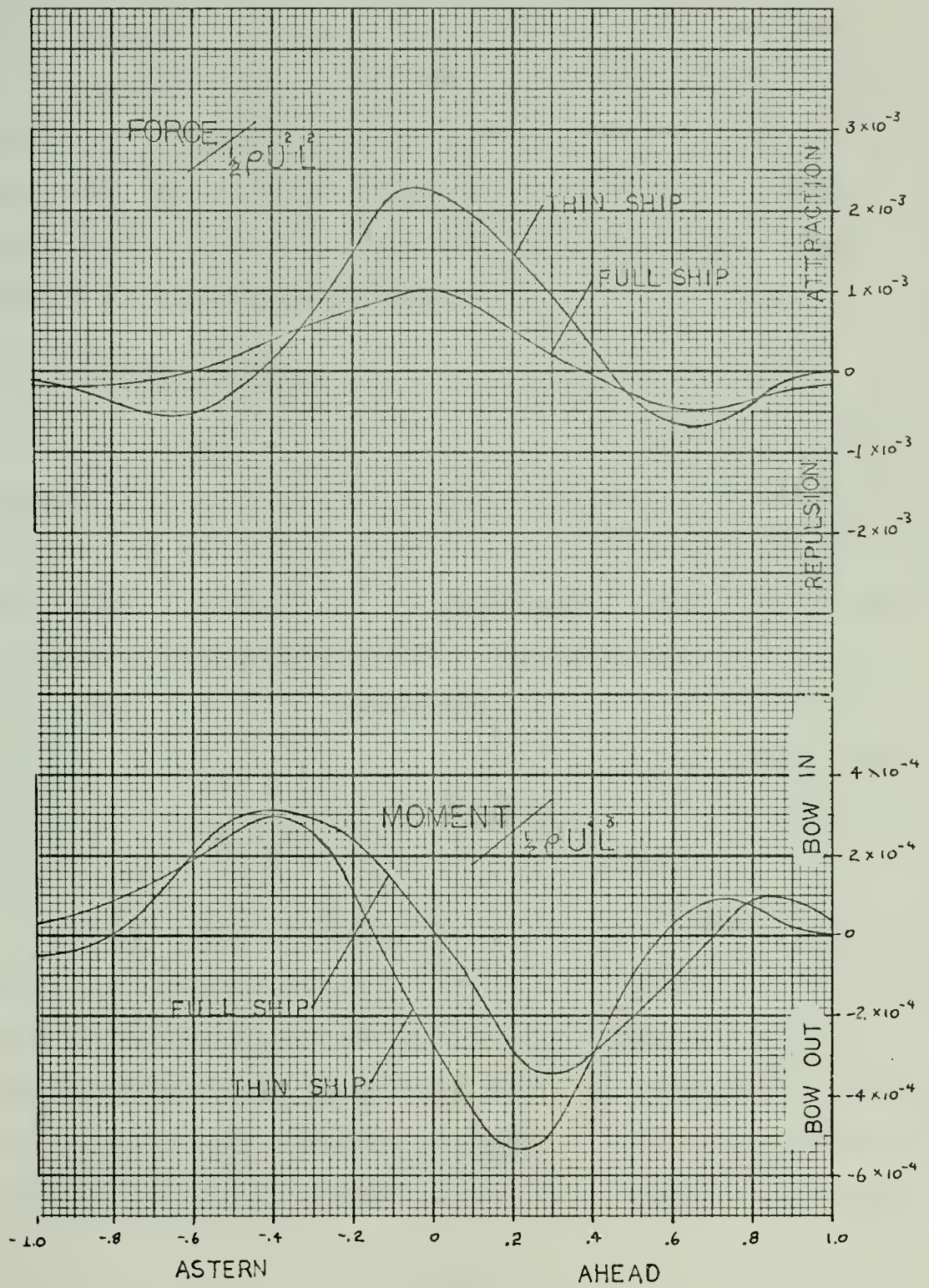

model length. The attraction and repulsion forces are self-explanatory and are applicable for the model passing on the starboard and port side. The moments are depicted as being either bow in or bow out. This indicates the direction in which the moment is acting on the model. The Thin Ship data represents Model Number 834 as it passes Model Number 838. The Full Ship data represents Model Number 858 passing Model Number 866.

1.2.3 Newton Results

Experiments were carried out at the Admiralty Experimental Works (AEW), Haslar, England, between 1946 and 1948 to test out the feasibility of the replenishment of warships with fuel tankers. These results were reported at the first Symposium on Ship Maneuverability at the David Taylor Model Basin in Washington, D. C. in 1960 by R. N. Newton. The tests conducted included an experiment with constrained models of the Battleship H.M.S. KING GEORGE and the R.F.A. OLNA. (Ship A and B Respectively)

A.E.W. used freely propelled and controlable models to study the behavior during maneuvering alongside and breaking away. The work also contains some data resulting from tests conducted at sea with ships. The results are presented here for the constrained models. The force moment acting on each ship has been converted to a position amidship.

FIGURE 3

A.E.W. MODEL TESTS

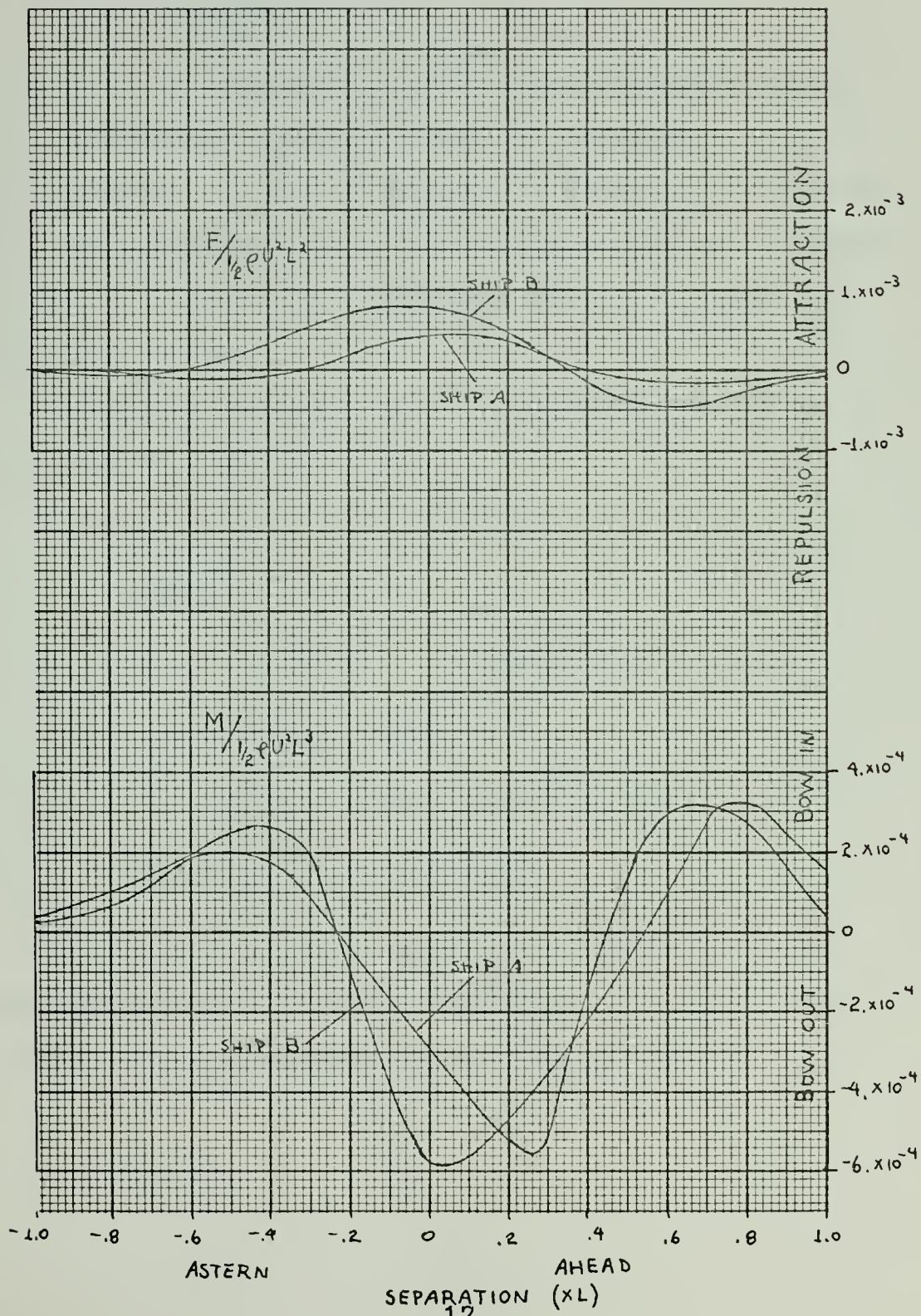

1.3 Previous Analytic Models

1.3.1 Ellipsoid

Sir H. T. Havelock proposed a model of ship interactions based upon potential flow. As an example, he cited the ellipsoid. In the discussion to Reference 8, the solutions were given for two unequally sized ellipsoids moving parallel in the fluid. The forces were calculated using Lagally's theorem.

The following singularity distribution describes an ellipsoid in a uniform flow.

$$SM(X) = 2 * C * V * X$$

WHERE

$$1/C = 4\,e/(1-e^2) - 2\log\left[(1+e)/(1-e)\right]$$

V = Speed in FT/SEC

X = Distance from midbody position

e= Ellipsoid eccentricity

Appendix D contains sample distributions for the ellipsoid model. Also, the results for the sample case cited by Havelock are recalculated in Appendix F.

1.3.2 Rankine Ovoid

The same model proposed by Havelock for use with the ellipsoid could be applied to any other body shape for which the singularity distributions are known. The Rankine Ovoid is one of the simplest bodies to generate from singularities in the fluid. It is formed by placing two equal but opposite singularities in a uniform flow so that their axis is in line with the incoming flow and the source is upstream of the sink. Given the singularities, it is easy to determine the size of the body that is represented in the fluid. Silverstein in Reference 14 developed the force on a Rankine Ovoid. Appendix F contains the recomputation of a case demonstrated in his paper. Even though the distribution is relatively simple and the body shape can be determined, it takes some effort to solve the inverse problem. The desired singularity strengths and positions for a given shape requires the simultaneous solution of two non-linear equations.

The following equations describe the Rankine Ovoid:

$$V = \frac{4.(\text{Strength})\ (\text{Dist})\ (L/2)}{[\,(L/2)^2 - (\text{Dist})^2\,]^2}$$

$$(B/2)^2 = \frac{4.\ (\text{Strength})\ (\text{Dist})}{V\ \sqrt{(B/2)^2 + (\text{Dist})^2}}$$

WHERE

V = Speed in ft/sec.

Dist = Distance from the modbody that singularities are located.

Strength = Singularity Strength

The solution of the simultaneous equations was accomplished on the computer using s system provided program called Zeroin. A copy of the instruction sheet for this program is included in Appendix H. A tabulation of Rankine Ovoid distributions is provided in Appendix D.

The experience with the system routine that solved the simultaneous equations should help future investigations. The Zeroin Program is one of two that were available. This particular one was selected mainly because it offered an automatic feature which permitted retrieval of intermediate steps in the solution so that the program results could be verified. It was found that an approximate solution to the problem using the semi-infinite body would provide a good starting solution for the program. The routine would not converge to the problem solution, however, until the magnitude of the initial solution vector was reduced in size by two orders of magnitude. This prevented the program from jumping past the solution and attempting to find another solution at very large values of the variables.

1.3.3 Slender Body Approximation

Newman has derived the forces and moments acting on a slender body of revolution moving parallel to a wall. In his derivation, it was assumed that the fluid was ideal and of infinite extent, thus ignoring any free surface affects.

In order that the boundary condition at the wall be satisfile, an image singularity distribution was provided. This is analogous to two bodies of revolution moving parallel and abreast through an infinite ideal fluid.

The approach used was to determine the singularity distribution that would develop fluid boundaries representing the rigid body moving through the medium. The singularities were sized using a two dimensional model and then transformed to three dimensional by assuming that the body was slender ($r_o << L$). The location of the singularities was determined by satisfying the linearized boundary condition on the body surface. It was pointed out that for the body close to the wall, the singularity distribution could be approximated by a general bipolar distribution. This resulted in the singularities being placed along the length of the body in such a way as to be displaced from the center axis. This formulation requires the wall be close ($Z_o/L << 1$). The displacement of the singularities is described by the following formulas, where the displacement from the centerline axis is equal to ($Z_o - a$).

$$a^z = Zo^2 - r_o^2$$

Once the singularity distributions are known, the forces acting on the body are calculated using Lagally's theory. It is easy to verify that the singularity distribution remains within the body and thus is amenable to a

Lagally force calculation. The following diagrams show the distributions for a sample ship form.

The procedure developed the singularity distribution using a slender body assumption. The resulting force integrals were then modified. An approximation to the integral is based upon the assumption that the part of the integrand which represents the singularity as a function of length can be treated as a constant value.

Newman's work produced the following results for the problem.

$$F_z = -\pi \rho U^2 \int_{-L/2}^{+L/2} \left[r_0(x)\, r_0'(x) \right]^2 \left\{ z_0^2 - [r_0(x)]^2 \right\}^{-1/2} dx$$

$$M_y = \pi \rho U^2 \int_{-L/2}^{+L/2} \left[r_0(x)\, r_0'(x) \right]^2 \left\{ z_0^2 - [r_0(x)]^2 \right\}^{-1/2} x\, dx$$

WHERE Z_0 = Separation of the body axis from the wall
r_0 = Radial dimension at position X along the body

Newman also presented a sample case to demonstrate the results. The body was assumed to be an ellipsoid described in the following form:

$$r_0(x) = r_{0m} * (1 - 4\, x^2 / 2)$$

WHERE

r_{0m} = Maximum radius of the body
x = Longitudinal position measured from the midship station.

Substituting into the Force Equation,

$$F_z = -\,{}^4/_3 \pi \rho U^2 r_{om}^3 L^{-1} \left[Q_0(\xi) - Q_2(\xi)\right]$$

WHERE

Q_n is the Legender Function of the Second Kind.

AND $\xi = {}^{z_0}/_{r_0}$

AS $\xi \to 1$

$$F_{z\ MAX} = -2\pi \rho U^2 r_{om}^3 L^{-1}$$

The force integrals were evaluated for this case and the results presented as follows.

FIGURE 4

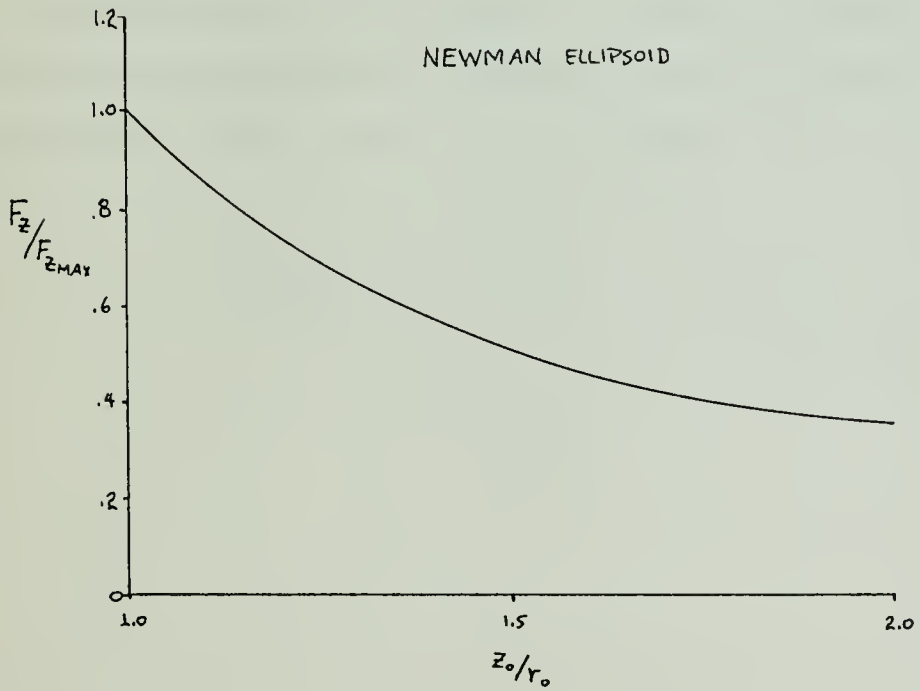

In the concluding comments of the paper, the author states, "....it seems likely that for bodies with full or blunt ends this [moment] integral will be dominated by the large values of S'(x) at the two ends, and thus the pitch moment will be positive (bow down) if the bow is blunt compared to the stern, and vice versa". In this comment, the pitch is analogous to the yaw in the previous defined orientations. He is predicting a 'bow out' condition if the sterns are blunt compared to the bows. The author also notes that the force is always attractive and "... for geometrically affine bodies, having the same cross sectional distributions but different lengths, the force will be inversely proportional to the length whereas the moment will be independent of the length". From this result, the nondimensional value of maximum force is inversely proportional to the cube of the L/B ratio.

$$F_{Z_{MAX}} / \tfrac{1}{2} \rho V^2 L^2 = 4\pi \left(\frac{B}{L}\right)^3$$

FIGURE 5

NEWMAN

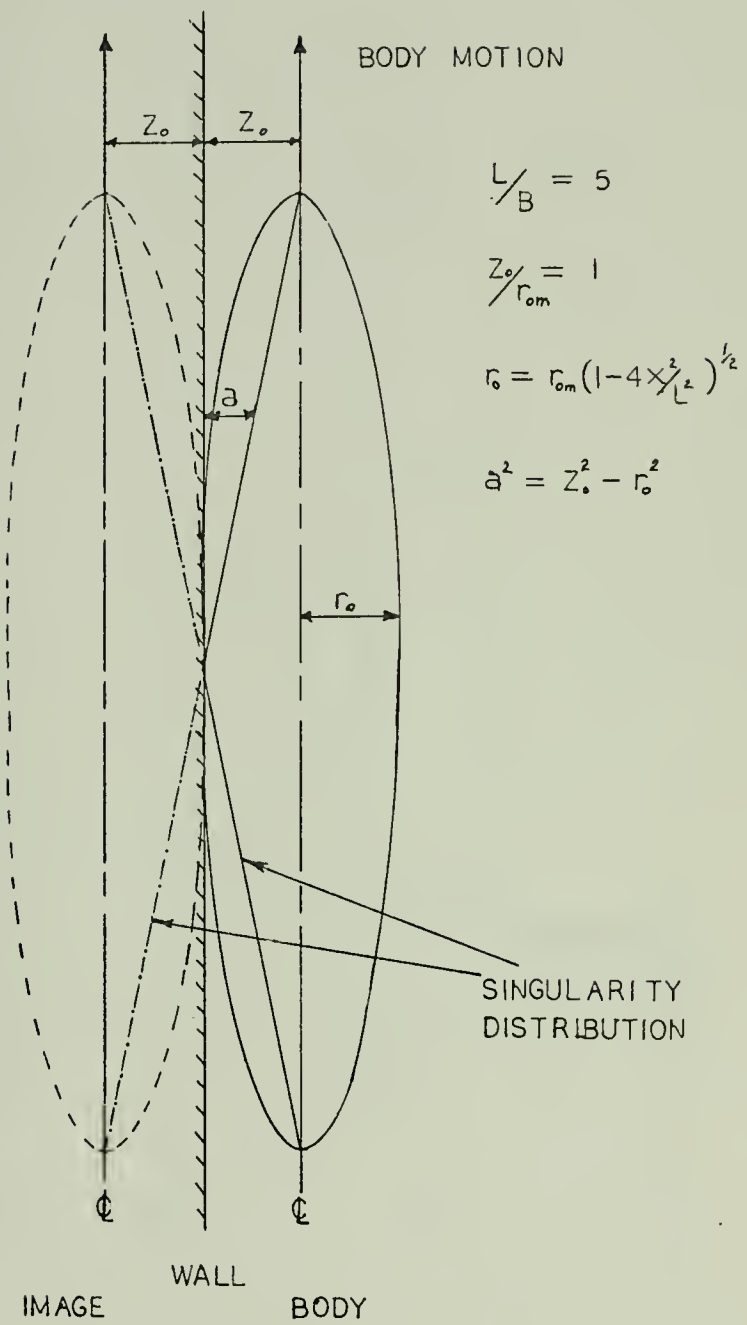

FIGURE 6
NEWMAN

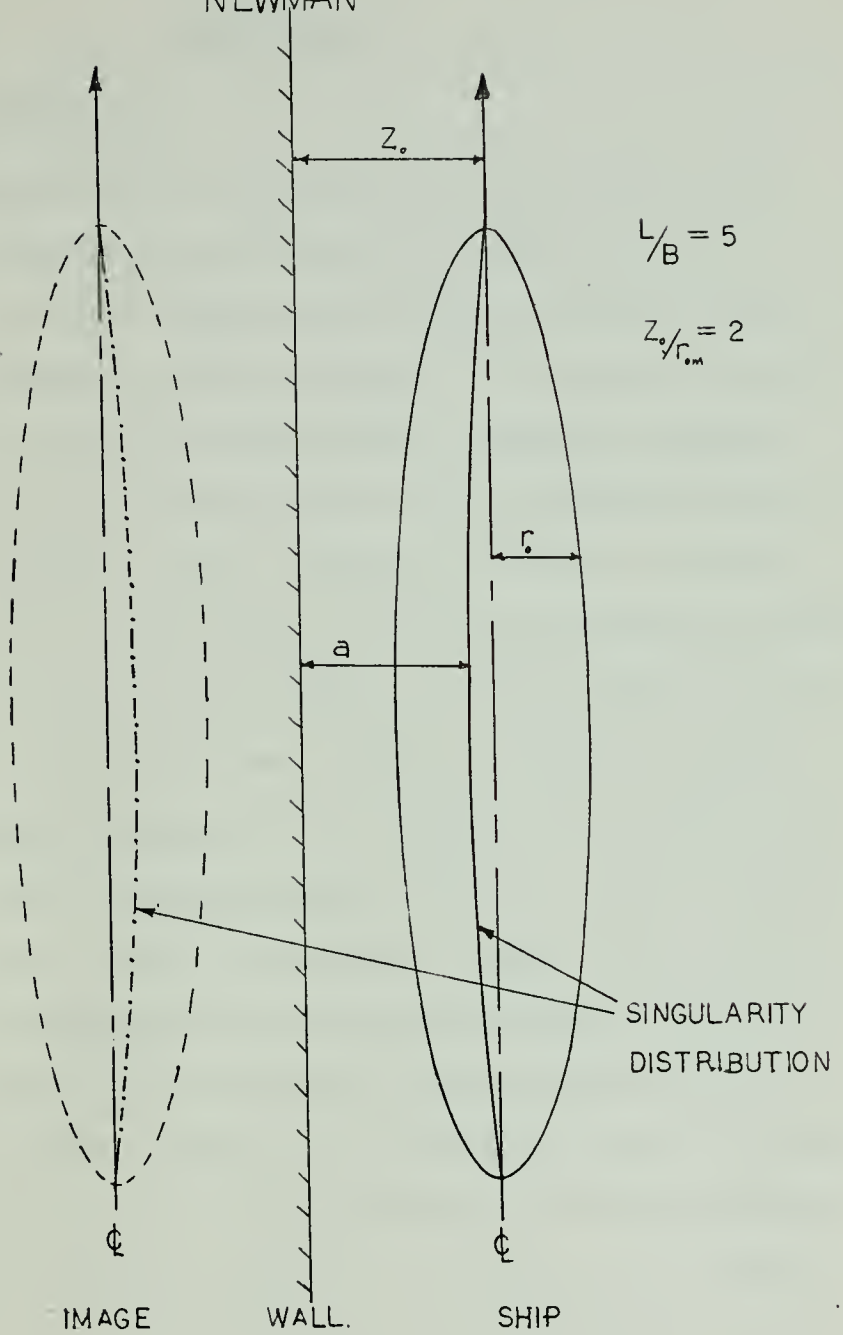

CHAPTER II.

FORCE MODEL

2.1 Model Description

The proposed model for predicting ship interaction forces uses the hypothesis proposed by Havelock that the potential field could explain the ship interaction phenomena. This approach seems reasonable for several reasons. First, the ship moving at the water's surface produces a flow field similar to that produced in an infinite fluid. Second, the potential field dominates the flow near the body. Pressures in this region fluctuate spatially and the changes find relief on the surface. The movement of this pressure field causes the wave system. Third, for most cases of interest, the ships are operating below their design speed. This is particularly true for naval ships replenishing at sea. The fine entry of these ships causes minimal wave disturbances when at replenishment speeds.

The potential flows without a free surface can be modeled using bodies moving in an infinite fluid with image systems to maintain the flow conditions on the waterline plane. This condition requires that there be no normal component of flow at the interface representing the undisturbed water level. A body of revolution moving horizontally in the fluid has a symmetry of flow and is used to model the ships. The maximum diameter of this body is taken

as the ship's beam because of the major influence this dimension has.

The force acting on the total body of revolution would represent twice the force experienced by the ship. The force results from the integration of pressures on (the lower) half of the body of revolution. The symmetry of flow will insure the same pressures and thus forces on the other half body.

The major reason for selecting a body of revolution was the ability of using an axial distribution of singularities to describe the flow. Hess et. al. have shown the computations required for representing an arbitrary body in an ideal fluid by a surface distribution of singularities. The computational effort for each ship would be much greater for surface distribution and as such is not desirable for use in a ship trajectory model.

In total, four models were developed and programmed. The first two incorporated the ellipsoid and Rankine Ovoid as discussed earlier. The third and final one involved a modified ellipsoid and slender body respectively, each with cross flow corrections. The first two used the derivations of Havelock and Silverstien. The third is only a special case of the fourth model. The slender body model will be discussed in more detail. Appendix I contains a logic flow chart of the computer program for this model.

The slender body model uses bodies of revolution to model the ships as described previously, the axial distribution of sources and sinks is obtained by assuming the body of revolution is slender. In two dimensions, the singularities are sized using the following equations. The derivation for three dimensions are presented in Appendix C.

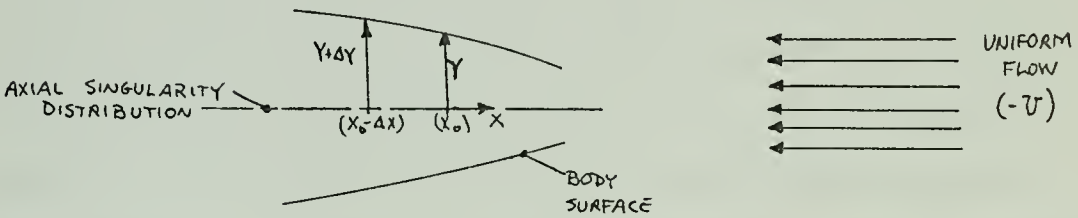

$$2\pi\, S_{2\text{-}D}(x_0) = \left.\frac{\partial Y}{\partial x}\right|_{x_0} * U$$

WHERE

$S_{2\text{-}D}(x_0) \equiv$ SOURCE STRENGTH PER UNIT LENGTH

$U \equiv$ FLOW MEASURED IN FT./SEC.

This axial distribution of singularities determines the body in a uniform flow. When another body comes near, the flow field is changed, so that it is no longer uniform. As the bodies approach each other, their affect in altering the flow field causes a deformation in the fluid boundary which describes the rigid bodies. To handle this problem an additional distribution of dipole singularities are placed along the axis. Thes· are oriented in the plus or minus direction on the body axis and are sized to counter

the effects of local cross flow on the bodies. The change in the flow in the axial direction is handled by perturbing the original singularity distribution.

The boundary condition on each body gives no flow across the boundary which describes the rigid body. In our case, this is a body of revolution. At each location along the body there is a radial distance at which the velocity (radial) must be zero. If the cross flows were uniform, the motion of an infinite cylinder could be represented exactly in the fluid by placing the appropriate doublet distribution on the axis. The flow pattern around a slender body of revolution can be approximated locally by an infinite cylinder because the change in diameter would be small for a change in the axial direction. For the distances between bodies of interest, it was estimated that the uniform flow assumption for any one segment of the body would be nearly correct. The dipoles were sized with flow of the value experienced on the body axis as a measure of the uniform flow strength. For the actual flow conditions, the boundary location is not calculated. It is assumed that the deviation from the exact position would be small. The dipole distribution is sized by the following rule. See Appendix C for derivation.

$$SD_{3\text{-}D}(X) = -2 * V(x) * AREA(x) / 4\pi$$

WHERE AREA ≡ CROSS SECTIONAL AREA

V ≡ CROSS FLOW VELOCITY IN FT/SEC.

If the perturbed flow is known, the changes in the singularity distribution can be readily determined. For the case of two bodies near each other, the change in the singularity distribution in one of the bodies is reflected in a slight change in the perturbed flow field experienced by the others. What is desired is a simultaneous solution to the problem. This is achieved by performing several iterations of the flow. Taking first one, than the other body, change its singularity distribution to counteract the perturbed flow, and then determine the resulting affect on the flow field at the other body. Changes in the perturbed flow were insignificant after about three to five iterations except when the bodies were etremely close and then it took only about ten iterations to achieve convergence to the solution.

2.2 Interaction Force Calculations

The interaction forces acting on a rigid body moving in an ideal fluid without viscosity can be determined if the fluid velocity field can be represented by a potential

function. In principle, the method for determining a force on any body would involve the calculation of the pressure on the body surface followed by the integration to obtain the total force. This was first accomplished by either Munk or Lagally for bodies generated with singularities. Lagally noted that for a body placed in a steady stream this integration took a form that would be analogous to a derivation which treats a force as acting between the singularities. The apparent force between a pair of singularities is determined in three dimensions by the following formula.

$$F_{12} = 4\pi\rho m_1 m_2 / r_{12}^2$$

Where a positive force indicates an attraction.

The total force would be determined by adding all pair contributions. The force acting on a body which is represented by a continuous source distribution along its axis has the following integral form.

$$F = 4\pi \int_{a'}^{b'} \int_{a}^{b} \frac{m(x)\, m'(x')}{[r(x,x')]^2} \, dx\, dx'$$

Where $[a,b]$ and $[a',b']$ indicate the line segments with singularities.

The results of Lagally were expanded by Cummins to include the forces between doublet singularities for the general time dependent case. His derivation involved the

following assumptions.

1. The velocity field is irrotational and has a velocity potential $\bar{\Phi}(x,y,z,t)$

2. If the body were not present, the stream would have a velocity potential ϕ, which we call the potential of the "undisturbed stream".

3. There are no singularities of the undisturbed stream in the region occupied by the body.

4. The boundary condition at the surface of the body is satisfied by superimposing a system of singularities upon the undisturbed stream, such singularities falling within the region which the body would occupy. The potential of the system of singularities is designated by ϕ_b. Then

$$\bar{\Phi} = \phi + \phi_b$$

Cummins found that the forces and moments calculated were of the same form as expressed in the Lagally derivation, but with additional terms. He expressed the Lagally force term as a product between local singularities and the total flow perturbation rather than as the sum of individual contributions from each singularity. The two representations for the force are identical. Zucker gives a summary of the results and indicates the contribution by Landweber and Yih in substantiating Cummins' results and evaluating the moment term resulting from the change in the fluid flow with time.

The force on the body will be as follows for Cummins' assumptions.

$$\vec{F} = \rho \forall \frac{d\vec{V}_o}{dt} + \vec{F}_1 + \vec{F}_2 + \vec{F}_3$$

$$\vec{M} = \rho \left[\vec{r}_g \times \frac{d\vec{V}_o}{dt}\right] \forall + \vec{M}_1 + \vec{M}_2 + \vec{M}_3$$

WHERE

$\forall$ = Volume of the body

V_o = Is the translational velocity of the body

$\vec{r}_g$ = Is the location of the centroid of the body relative to the origin of the moving system.

F_1 = The force if the body were not rotating and the undisturbed stream were steady (Lagally Force)

F_2 = Force due to change of the flow with time

F_3 = Force arising from body rotations

M_1 = Moment if the dlow were steady (Lagally)

M_2 = Moment due to the flow changing with time

M_3 = Moment effect due to rotation of the body

FOR SITUATIONS DESCRIBED BY ONLY SOURCES AND DOUBLETS, F_3 AND M_3 ARE ZERO.

FOR A SOURCE OF STRENGTH

$$\vec{F}_1 = -4\pi \rho m \vec{q}'$$

WHERE $\vec{q}'$ defines the fluid velocity in the undisturbed stream

$$\vec{F}_2 = -4\pi \rho \frac{d}{dt}(\vec{r} m)$$

$$\vec{M}_1 = \vec{r}_g \times \vec{F}_1 = -4\pi \rho m (\vec{r}_g \times \vec{q}')$$

FOR A DOUBLET OF MOMENT

$$\vec{F}_1 = -4\pi \rho (\vec{\mu} \cdot \vec{\nabla}) \vec{q}'$$

$$\vec{F}_2 = -4\pi \rho \frac{d}{dt}(\vec{\mu})$$

$$\vec{M}_1 = \vec{r}_g \times \vec{F}_1 + 4\pi \rho (\vec{q}' \times \vec{\mu})$$

NOT EVALUATED BY CUMMINS ARE THE MOMENT DUE TO THE FLOW CHANGING WITH TIME.

$$M_2 = \frac{d}{dt} \int_S (+\rho) \Phi (\vec{r} \times \vec{n}) \, d\sigma$$

WHERE: $\vec{n} \equiv$ INWARD DIRECTED NORMAL VECTOR

This term was evaluated by Landwebber and Yih.

The force calculations programmed on the computer used at least one of the forms discussed previously. As more complicated and detailed models were developed the form of the force calculation was selected to improve computational efficiency. For the Rankine Ovoid and ellipsoid which do not contain cross flow corrections, the simplest statement of Lagally's force was used. When it became necessary to introduce dipoles to correct for the cross flow, the final form of Cummins was used. The final slender body model takes into account the terms that are represented by $\vec{F}_\perp$ and $\vec{M}_\perp$. This represents the non-zero terms of the interaction force for steady parallel motion of the bodies.

The above equations relate to a three dimensional flow problem. The two dimensional case is similar with the Lagally force being of the following form:

$$F_{12} = 2\pi\rho\, m_1 m_2 / r_{12}$$

Havelock developed in Reference 7 the force and moments acting on a two dimensional body by using contour integration.

FOR SOURCE DISTRIBUTION

$$\vec{X} = 2\pi\rho \sum_{(r,s)} m_r m_s (X_s - X_r) / R_{rs}^2$$

$$\vec{Y} = 2\pi\rho \sum_{(r,s)} m_r m_s (Y_s - Y_r) / R_{rs}^2$$

WHERE

1. Suffix "S" refers to the given distribution in the liquid, and "r" to the image system within the surface of the body.

2. Summation extends over the external and internal sources taken in pairs.

FOR DIPOLE DISTRIBUTION

$$\vec{X} = \sum_{(r,s)} \vec{X}_{rs} = -4\pi\rho \sum_{(r,s)} M_r M_s \cos(\alpha_r + \alpha_s - 3\theta_{rs}) / R_{rs}^3$$

$$\vec{Y} = \sum_{(r,s)} \vec{Y}_{rs} = +4\pi\rho \sum_{(r,s)} M_r M_s \sin(\alpha_r + \alpha_s - 3\theta_{rs}) / R_{rs}^3$$

Where: — the doublet is of moment M and makes an angle α with the x axis (ship).

And: θ_{rs} being the angle between x' and the vector drawn from the doublet (r) to the doublet (s).

The total moments results from moments of forces already determined plus an additional term.

$$M' = 2\pi\rho \sum M_r M_s \sin(\alpha_r + \alpha_s - 2\theta_{rs}) / R_{rs}^2$$

2.3 Computation

The earlier discussion of the slender body model gave the general steps involved for determining the interaction forces. In this procedure there were two major areas requiring considerable effort. First, it was necessary that derivatives of the flow potentials be derived for the force calculations. These potentials and their derivatives were defined in terms of a moving axis system of the ship in which the forces were acting. The necessary transformations and derivations are developed in Appendix B.

The second area involved the determination of the total force acting on the ship. The slender body was defined by a continuous distribution of singularities. The resulting flows in the fluid were determined by integrating the contributions from the singularity distribution. Also the forces were determined by integrating the individual force contributions. In both cases, the numerical integration used values of the integrand at the same location on the body axis. These coincided with the stations at which the sectional area curve had been defined. The integration was performed in each case using Simpson's Rule with an odd number of stations (21), evenly spaced along the body axis.

CHAPTER III.

COMPARISON OF RESULTS

3.1 Taylor Model Tests

The Rankine Ovoid and ellipsoid models were developed and checked with the available results then used to model the forces and moments reported by Taylor. Figure 7 depicts the results. These predictions differ in two ways with Taylor. First, they do not predict the secondary reversal in the moment that is evident at longitudinal separations of .6×L. Secondly, the largest moment is predicted for longitudinal separations above 1.0 × L. This variation can be attributed to the deformation of the boundaries of the bodies as they approach each other. If the boundary was maintained in the original position, the flow would have been restricted, thus increasing the fluid velocity and contributing to a lower pressure on the bodies. This reduction in pressure would contribute a moment that would cause a reversal in sign. The inability of the previous theoretical models to explain the reversal in sign of the moment curve, led to the development of a model which incorporated cross flow corrections. The correction for cross flow indicates the reversal in the moment can be modeled. However, the magnitudes were not in full agreement with those obtained by Taylor. Computations were made

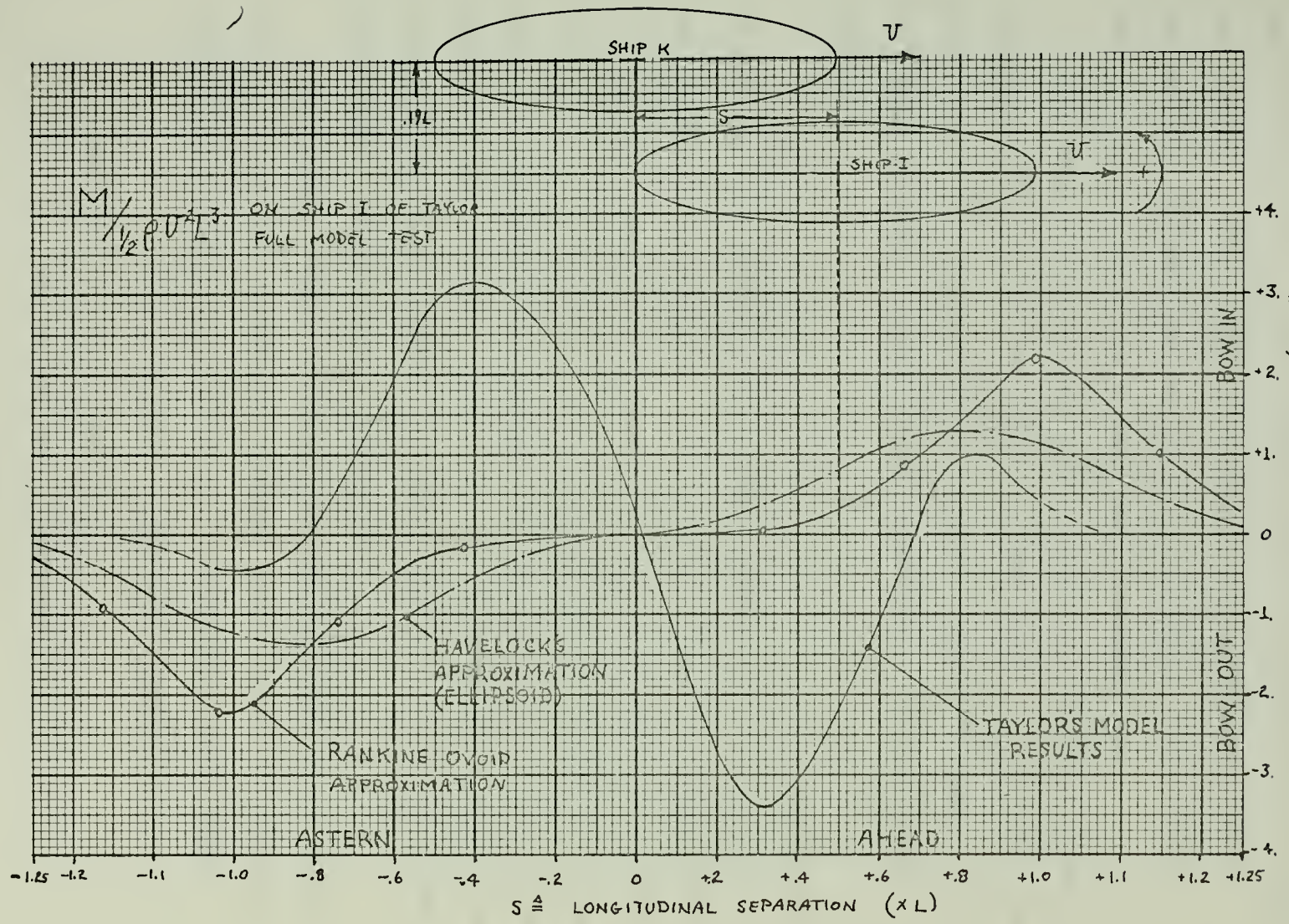
SHIP K
V
.19L
S
SHIP I
V
$M/\frac{1}{2}\rho V^2 L^3$ ON SHIP I OF TAYLOR FULL MODEL TEST
HAVELOCK'S APPROXIMATION (ELLIPSOID)
RANKINE OVOID APPROXIMATION
TAYLOR'S MODEL RESULTS
ASTERN
AHEAD
BOW IN
BOW OUT
MOMENT COEFFICIEN (X10⁻⁴)
+4. +3. +2. +1. 0 -1. -2. -3. -4.
-1.25 -1.2 -1.1 -1.0 -.8 -.6 -.4 -.2 0 +.2 +.4 +.6 +.8 +1.0 +1.1 +1.2 +1.25
S ≙ LONGITUDINAL SEPARATION (X L)

FIGURE 7

at higher speeds with no variation in the results. This was expected, the plot involved the non-dimensional moment coefficient. For closer distances, the predicted amplitude of the moments increased only slightly. (The model tests were conducted at a very small separation.)

The dimensions of the models used in Taylor's experiments were inputs to the slender body model. Calculations were made for the same cases as described by Taylor. The following curves show the results plotted for comparison purposes.

Additional curves are drawn which show the forces predicted for the Taylor full bodied models, as the lateral separation is increased. The reversal in moment diminishes as the ships separate because there is no longer a restriction in the flow to cause a pressure drop between the ships. Beyond a distance of 2 beams, the results agreed with those obtained with a model which did not incorporate cross flow corrections. Only beyond a separation of 4 beam widths interaction effects were negligable.

The model tests conducted by Taylor, and the slender body predictions differ in several ways. Some of the more significant assumptions used for the slender body were:

1. The potential field was assumed most important (No free surface)
2. The ships were represented by a body

FIGURE 8

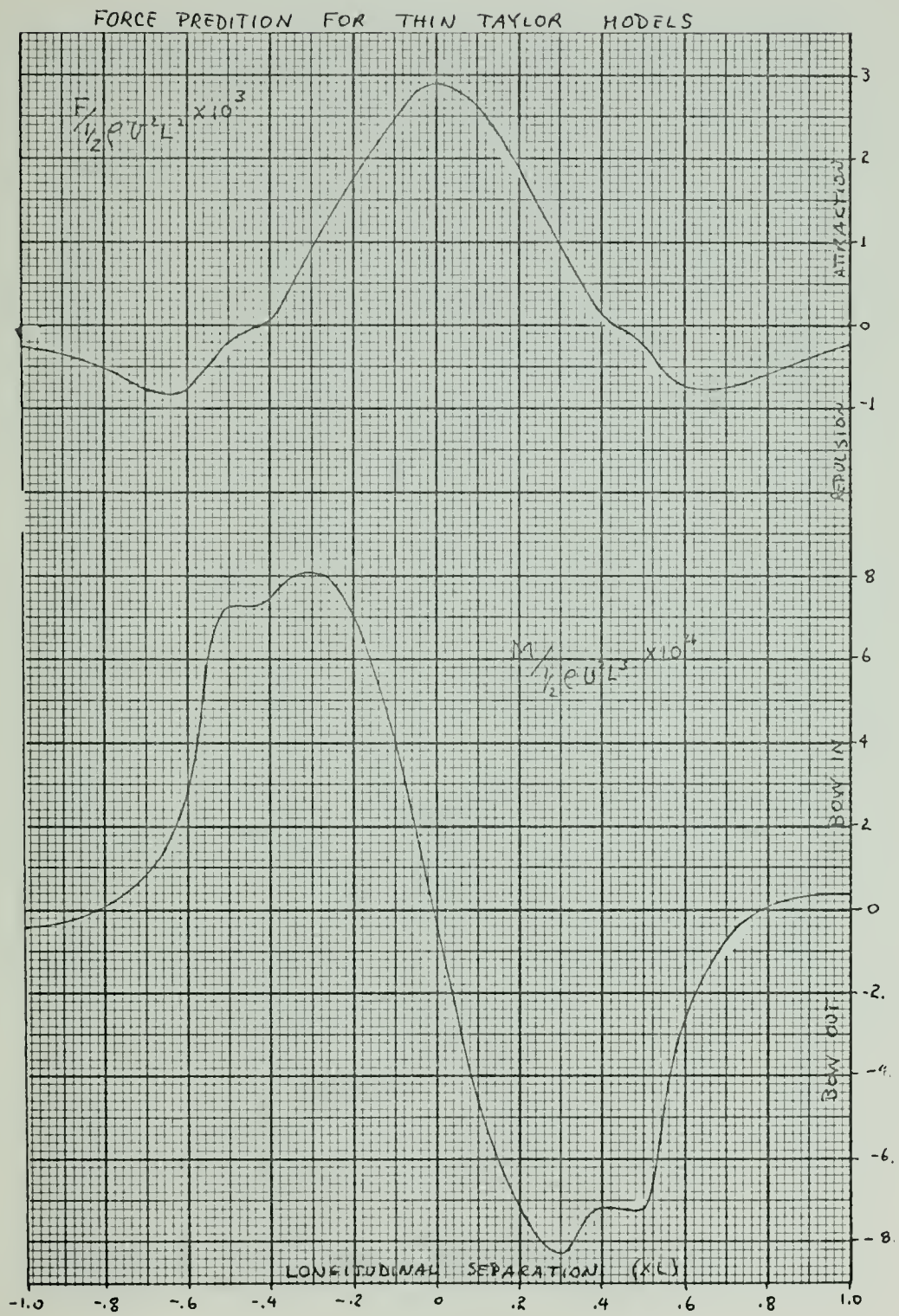
FORCE PREDITION FOR THIN TAYLOR MODELS
F/½ρU²L² X10³
M/½ρU²L³ X10⁴
ATTRACTION
REPULSION
BOW IN
BOW OUT
LONGITUDINAL SEPARATION (X/L)
3
2
1
0
-1
8
6
4
2
0
-2.
-4.
-6.
-8.
-1.0
-.8
-.6
-.4
-.2
0
.2
.4
.6
.8
1.0

FIGURE 9

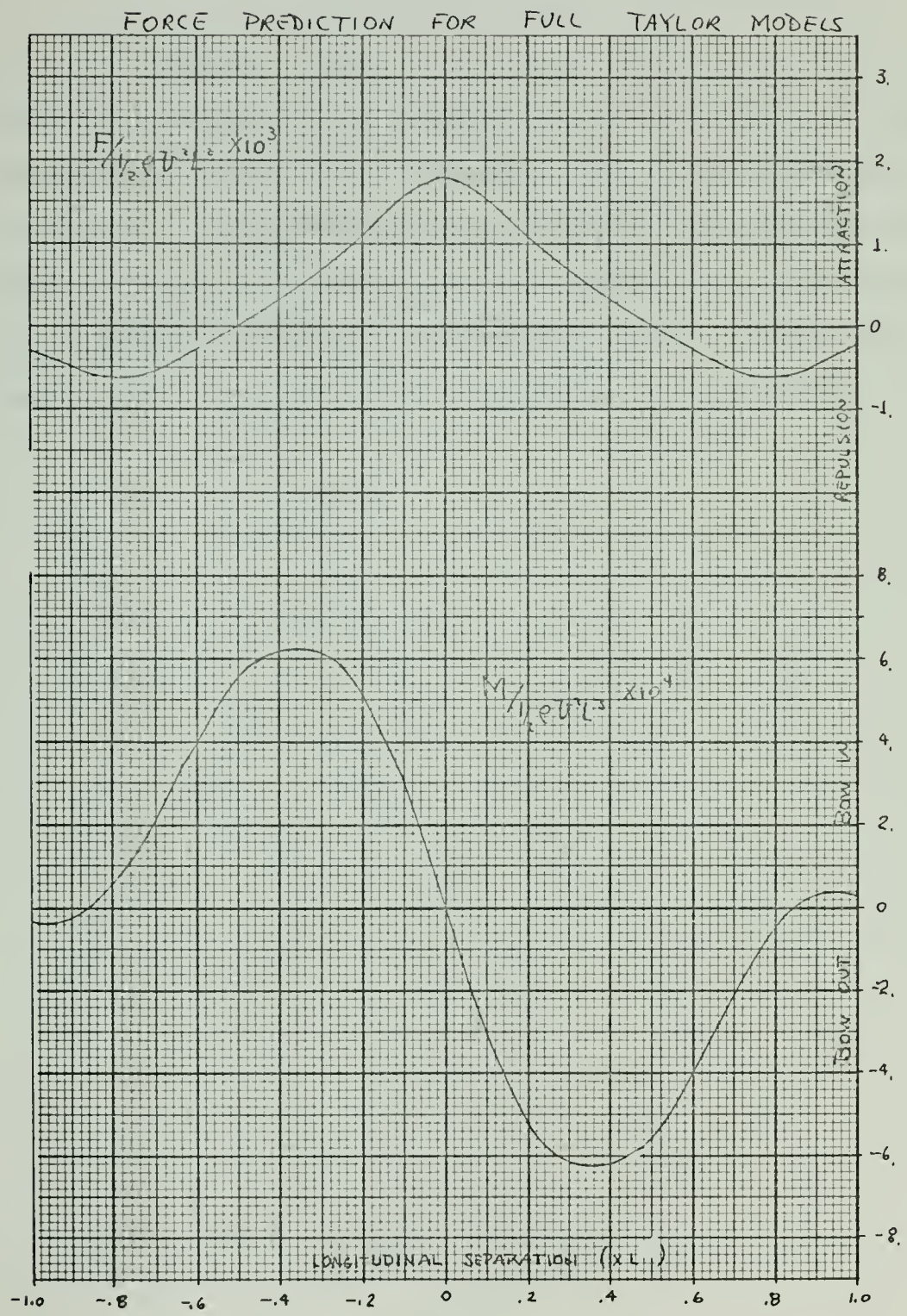
FORCE PREDICTION FOR FULL TAYLOR MODELS
$F/\frac{1}{2}\rho U^2 L^2 \times 10^3$
$M/\frac{1}{2}\rho U^2 L^3 \times 10^4$
ATTRACTION
REPULSION
BOW IN
BOW OUT
3.
2.
1.
0
-1.
8.
6.
4.
2.
0
-2.
-4.
-6.
-8.
LONGITUDINAL SEPARATION (X L)
-1.0
-.8
-.6
-.4
-.2
0
.2
.4
.6
.8
1.0

of revolution. (Lessen effective beam)

3. Squat and sinkage were not incorporated.

Other differences in the results may be attributed to either asemmetry in the models or inaccuracies in the measurement techniques. The apparatus used by Taylor was not indicated. When the tests were conducted, the resistance measurements used a system of weights, pulleys and levers. Taylor even commented on the problem of conducting the model tests.

3.2 Comparison of Results with Newman

In order that a comparison be made between the model developed and the results of Newman. The sample problem in Newman's paper was used. The sectional area curve for the ships moving in parallel were determined using the radius formula presented earlier. Two ships moving in parallel were defined with the same geometry. The initial calculation assumed a length of 600 feet, a beam of 100 feet and a speed of 10 knots. The lateral displacement was determined and plotted according to the non-dimensionalization used by Newman.

Note that Z_o/r_o is equivalent to the separation distance between the axis of the two bodies divided by their beam dimension. Other beam to to length ratios were calculated by varying the length of the bodies while maintaining the beams constant. These included the L/B of 6, 10, 20, 60. The total force on the body of revolution determined using the model was non-dimensionalized by the maximum value determined by Newman. The following graphs depict the results developed in this thesis.

The first graph shows the results for a L/B of 6 for the various theoretical models. Calculations were then made for the resulting forces with and without the cross-flow correction which used the dipole distribution. It was expected that the results of Newman and the proposed

FIGURE 10

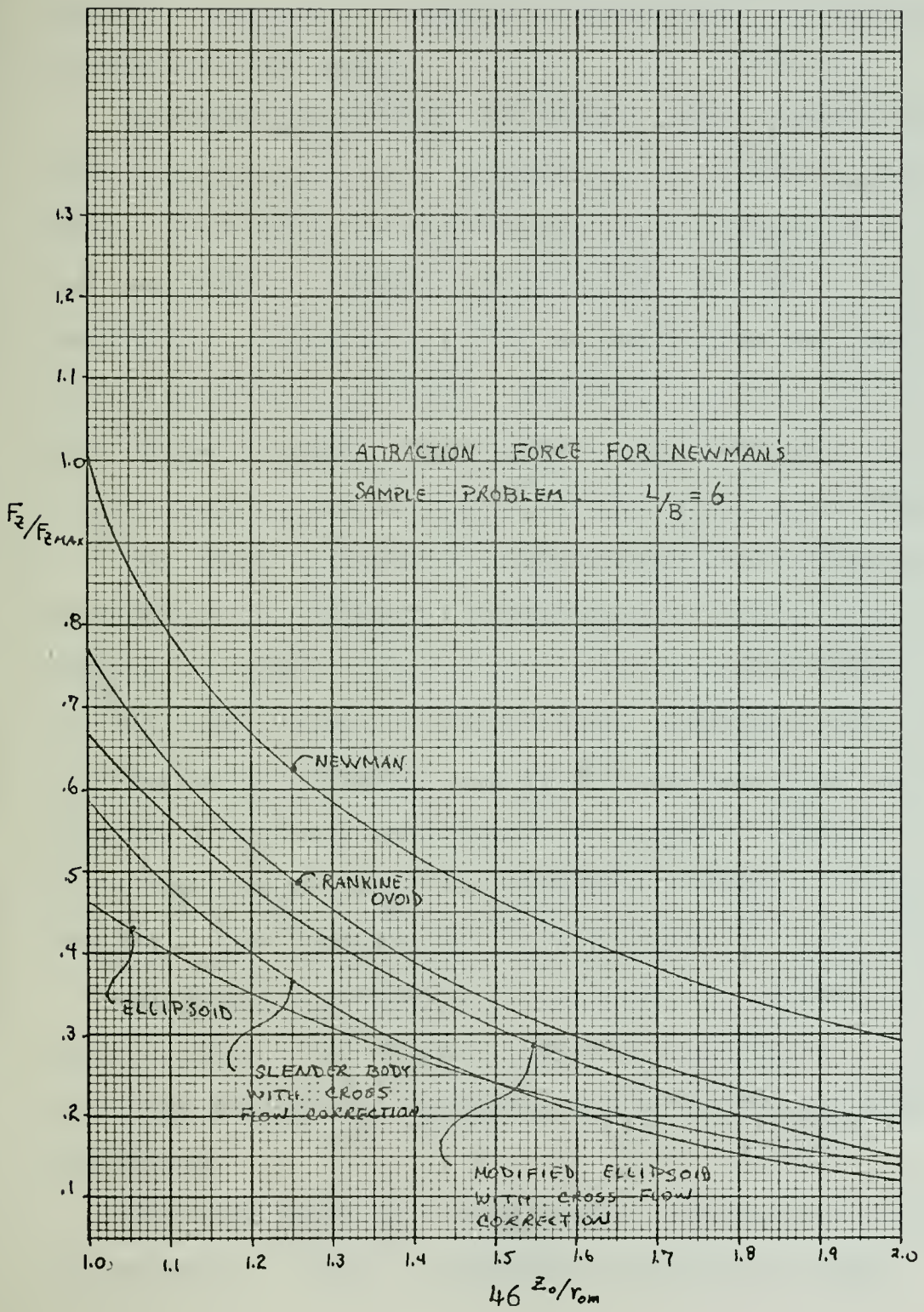
ATTRACTION FORCE FOR NEWMAN'S SAMPLE PROBLEM L/B = 6
F_Z/F_ZMAX
1.3
1.2
1.1
1.0
.8
.7
.6
.5
.4
.3
.2
.1
NEWMAN
RANKINE OVOID
ELLIPSOID
SLENDER BODY WITH CROSS FLOW CORRECTION
MODIFIED ELLIPSOID WITH CROSS FLOW CORRECTION
1.0
1.1
1.2
1.3
1.4
1.5
1.6
1.7
1.8
1.9
2.0
46 Z_o/r_om

model would approach each other in the limit of high L/B ratios and for very slender bodies because the singularity distributions would be nearly identical and lie very close to that used by Newman.

The next graph shows the change in the non-dimensionalized maximum force as a function of the length to beam ratio. Note that the singularity model approaches the Newman result in the limit. On the graph, the error of the computation is indicated. The solution with the dipole correction seems to converge initially and then for very high ratios diverge. This tends to indicate that the dipole correction may be useful for all ratios of interest.

The error introduced during integration was easy to approximate for the axial distribution of singularities because the fourth derivative of the integrand should be exactly zero. However, for the case with the dipole cross flow correction this may not be the case and it is expected that the introduced error would be larger. This may explain the divergence of the solution for high L/B (large lengths). See Appendix E. for derivation of error estimate.

Another graph shows more directly the variation in the results for the various length to beam ratios. In this graph the shaded area indicates the effect of the dipole correction.

The last graph is a compilation from various sources of interaction forces. They are plotted in the same

FIGURE 11

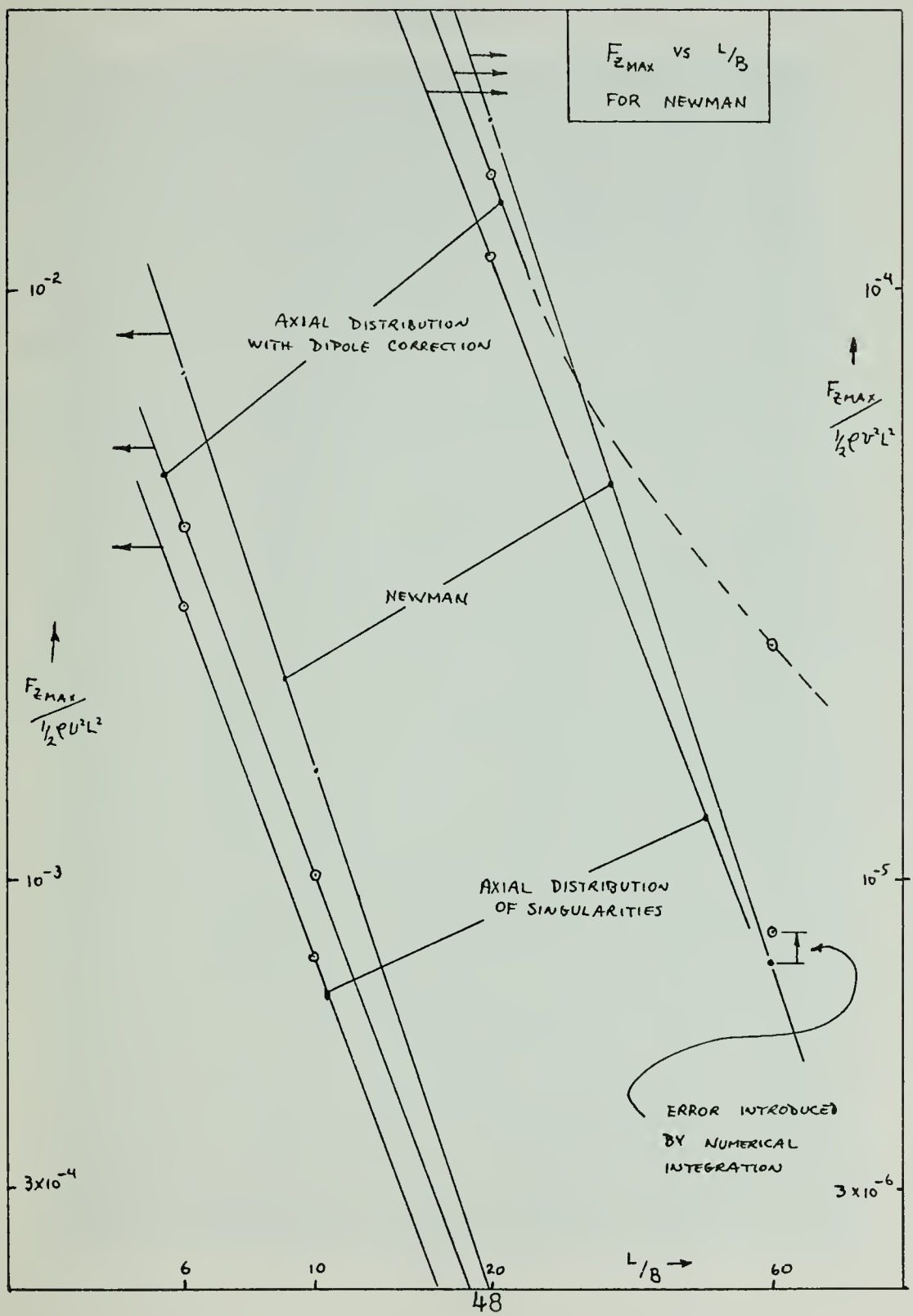
$F_{Z_{MAX}}$ VS L/B
FOR NEWMAN
10^{-2}
10^{-3}
3×10^{-4}
10^{-4}
10^{-5}
3×10^{-6}
$\frac{F_{Z_{MAX}}}{\frac{1}{2}\rho U^2 L^2}$
AXIAL DISTRIBUTION WITH DIPOLE CORRECTION
NEWMAN
AXIAL DISTRIBUTION OF SINGULARITIES
ERROR INTRODUCED BY NUMERICAL INTEGRATION
6
10
20
60
L/B

FIGURE 12

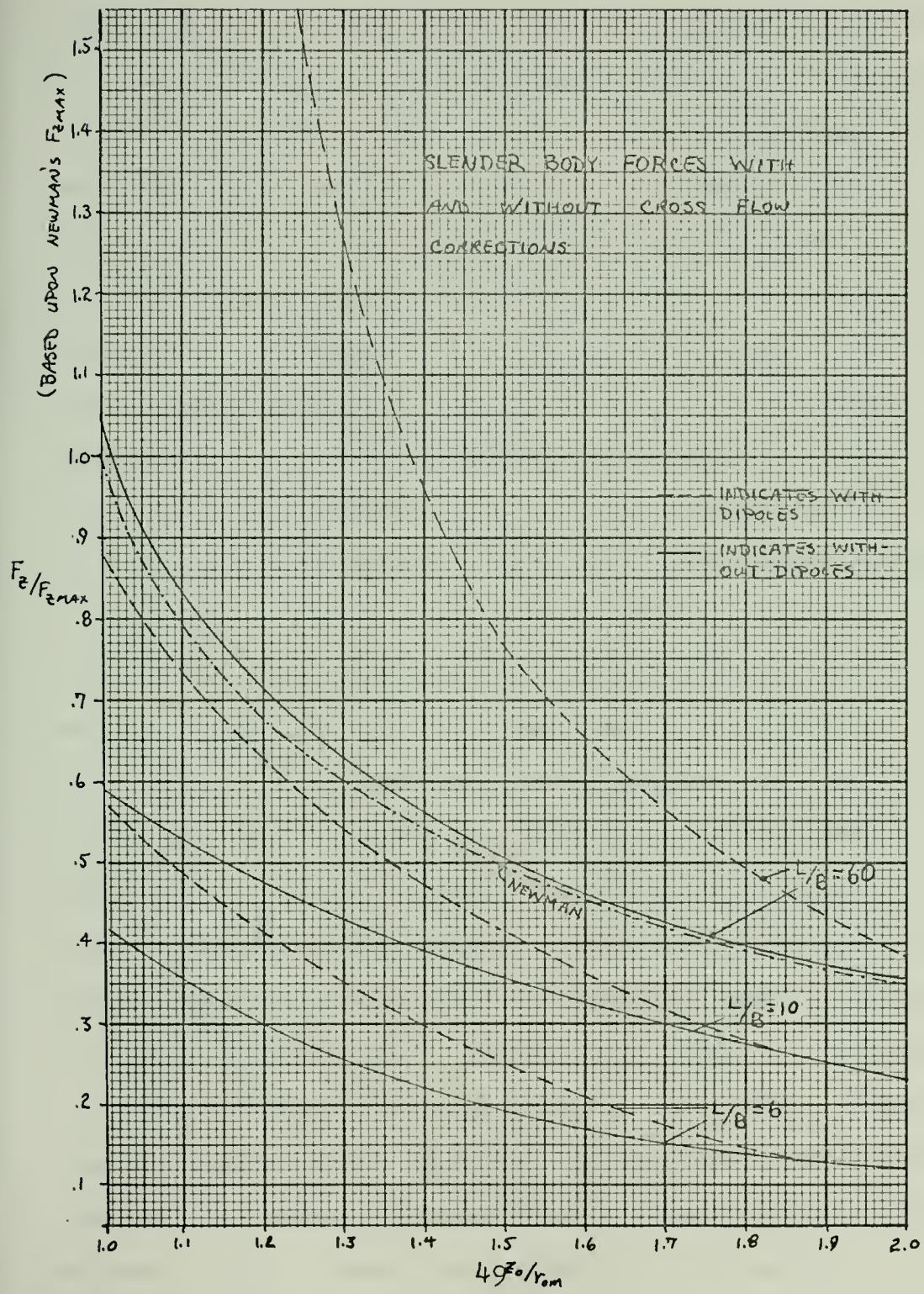
SLENDER BODY FORCES WITH AND WITHOUT CROSS FLOW CORRECTIONS
(BASED UPON NEWMAN'S $F_{z_{max}}$)
$F_z/F_{z_{max}}$
$4\pi z_0/r_{om}$
1.5
1.4
1.3
1.2
1.1
1.0
.9
.8
.7
.6
.5
.4
.3
.2
.1
1.0
1.1
1.2
1.3
1.4
1.5
1.6
1.7
1.8
1.9
2.0
INDICATES WITH DIPOLES
INDICATES WITHOUT DIPOLES
NEWMAN
L/B=60
L/B=10
L/B=6

non-dimensional terms. For the ships, the forces were doubled to approximate the forces that would be observed between bodies of revolution. The non-dimensionalization with respect to the maximum force predicted by Newman is consistant with the other graphs. Plotted also are the solutions predicted for a body of revolution with L/B ratios of 6 and 10 with the geometry used by Newman. The plot indicates that the model tests agree more closely to the results predicted by the proposed model with the results of the tests by Newton showing the greatest variation. If the results had been mislabeled the results would have been more consistant with the proposed model predictions.

The basic differences in the proposed model and that of Newman are, first, the surface condition on the body is accounted for by displacing the singularities from the centerline in the case of Newman, where the proposed model uses a dipole distribution. It is obvious that the proposed model will satisfy the surface condition better when the induced velocity is fairly uniform over the body profile. From the data presented, the relatively small L/B and the separation distances of interest justify the use of dipole corrections. A second difference in the models is in the evaluation of the integral solutions. Newman uses an approximation to the solution which emphasizes the need to restrict the solution to the slender bodies, whereas this model uses numerical integration.

FIGURE 13

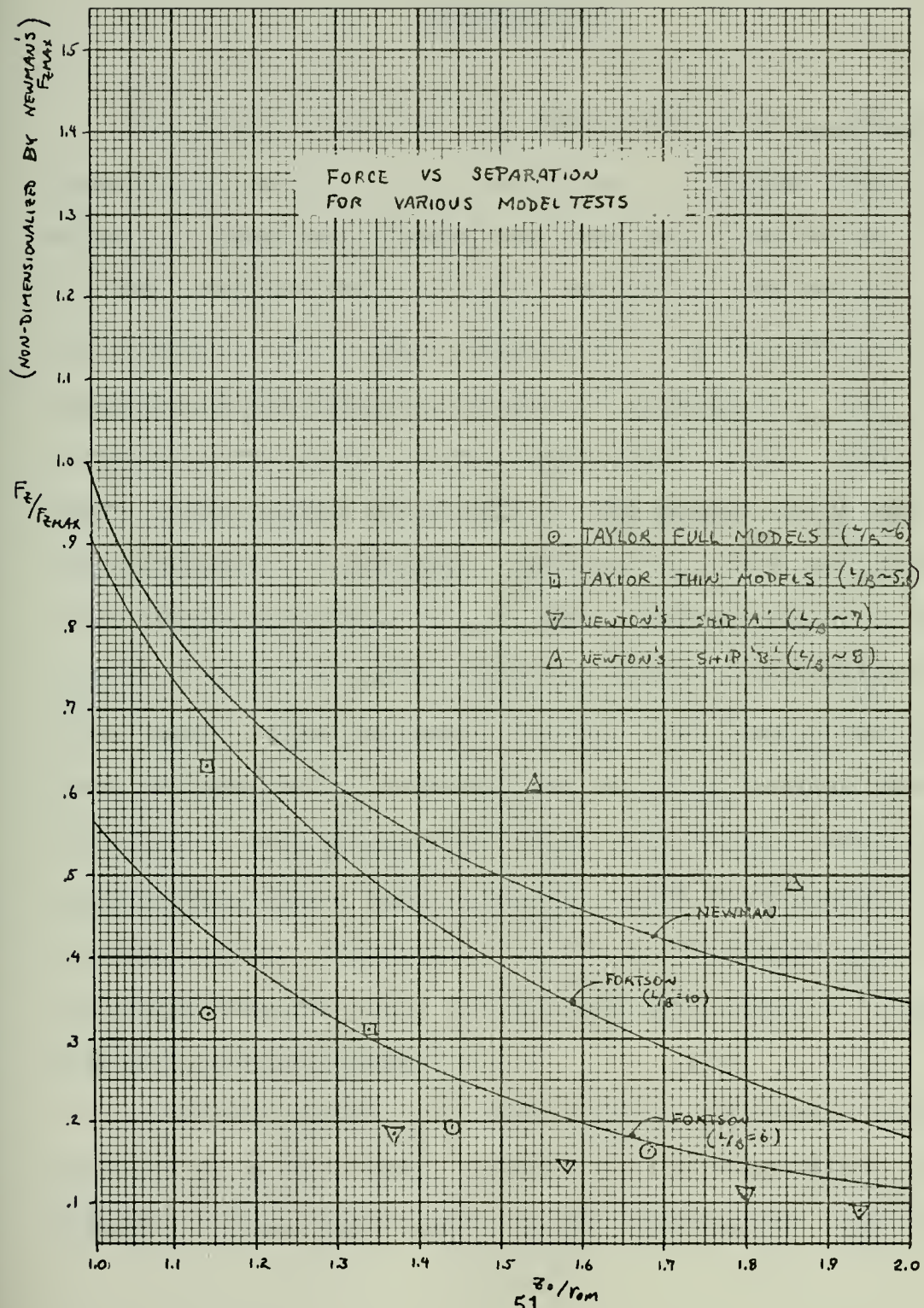
FORCE VS SEPARATION
FOR VARIOUS MODEL TESTS
(NON-DIMENSIONALIZED BY NEWMAN'S $F_{Z_{MAX}}$)
$F_z/F_{Z_{MAX}}$
1.5
1.4
1.3
1.2
1.1
1.0
.9
.8
.7
.6
.5
.4
.3
.2
.1
1.0
1.1
1.2
1.3
1.4
1.5
1.6
1.7
1.8
1.9
2.0
z_0/r_{om}
⊙ TAYLOR FULL MODELS ($L/B \sim 6$)
⊡ TAYLOR THIN MODELS ($L/B \sim 5.5$)
▽ NEWTON'S SHIP 'A' ($L/B \sim 7$)
△ NEWTON'S SHIP 'B' ($L/B \sim 8$)
NEWMAN
FORTSON ($L/B = 10$)
FORTSON ($L/B = 6$)

CHAPTER IV

CONCLUSIONS

The major effort of the thesis has been to provide a theoretical model for the prediction of forces between ships. A computer program has been developed which carries out the computations for ships in rectilinear motion using the potential flow model described. The ellipsoid model proposed by Havelock was unable to predict the form of the results as indicated by empirical model tests. These tests demonstrated a reversal in the moment force as the ship separation decreased. This led to the development of the slender body model with cross flow corrections. The programs which were developed for ships in rectilinear motion ignore time dependent forces. The data presented here represents the interactions of ships in deep water, on parallel courses and with each ship at the same speed. Orientation, other than parallel, would have resulted in a change in the relative positions of the ships with time and would involve other force terms as derived by Cummins, but were not programmed here.

The investigation of past efforts indicate a lack of good model or full scale data to test a theoretical result. The differences experienced in the analysis of Taylor's

results could not be fully explained without more empirical data. This can only be obtained with ship models because of the parallel course requirements.

In meeting the objectives of the thesis, the axial distribution of singularities and the force calculation techniques provide additional inputs to a general trajectory model. When the ship approaches other bodies or boundaries in the fluid, this work will help to predict the interactive forces so that more inclusive trajectory calculations can be made. This is applicable to the determination of the factors involved in ship collisions, the prediction of the control parameters for at sea replenishments, or for future ship design characteristics.

The performance of model tests may indicate results that differ from Taylor's. The design of model experiments must take into account the large forces introduced by any misalignment of the models. Also, the wall effects may introduce erroneous readings. The computer program has been written to include more than two ships in proximity. It could be used to estimate the wall effects in the tow tank experiments by introducing the first few image distributions to approximate the wall boundary conditions. The following figure shows the orientation. It will be important that some tests be repeated with the models in a reverse geometry to insure accurate readings. This would

FIGURE 14

THEORETICAL CALCULATION OF WALL EFFECTS ON INTERACTION FORCE MODEL EXPERIMENTS

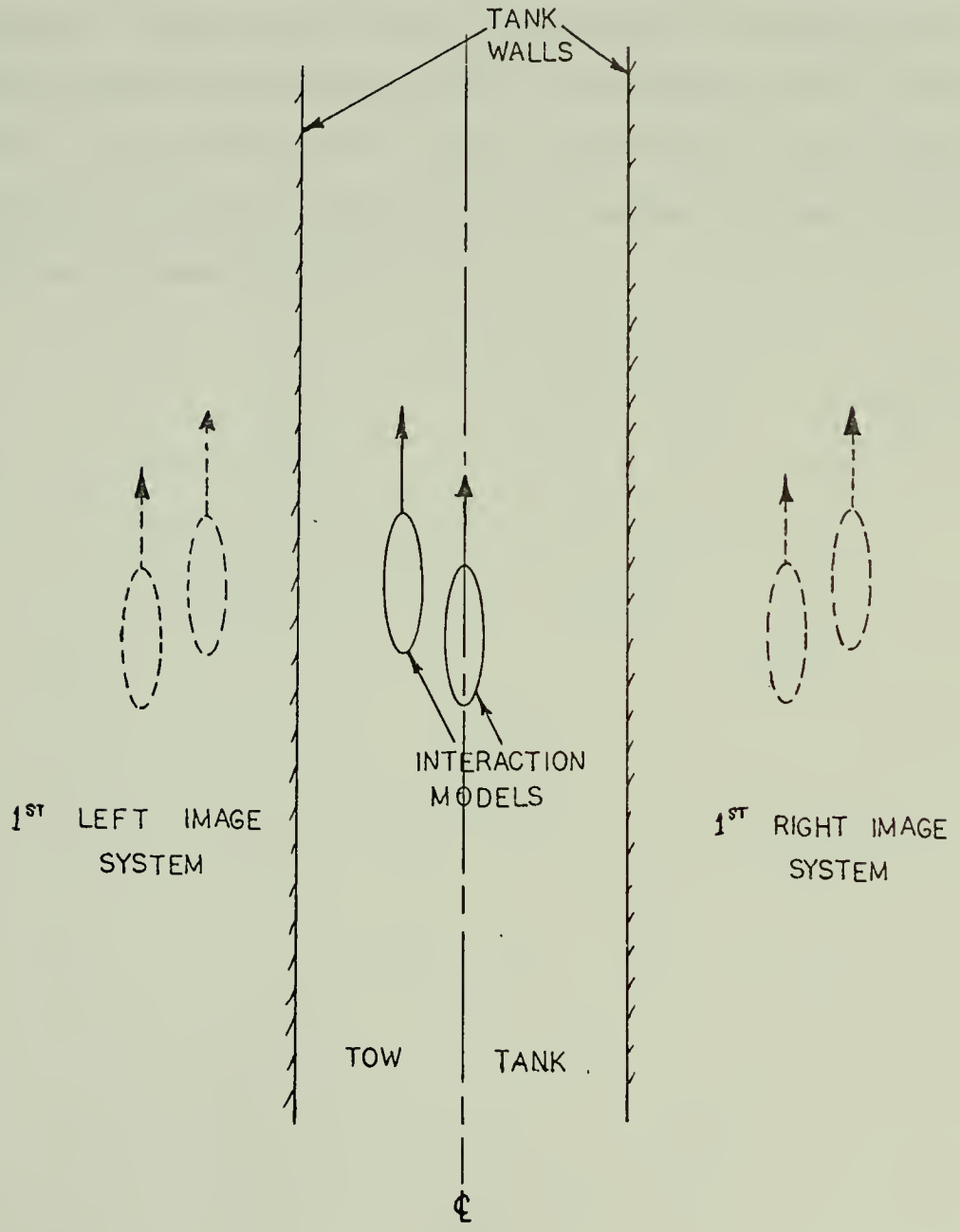

give a measure of the wall effects and asymmetries in the models.

The program can be extended to cover shallow water effects. For very shallow water, a two dimensional model could be developed by only a few changes in the present program. These would involve the change in sizing the singularity distributions and in the Lagally force calculation. For other shallow water conditions, the boundary conditions could be satisfied by a series of image distributions as shown in Figure 15.

FIGURE 15

SHALLOW WATER APPROXIMATION

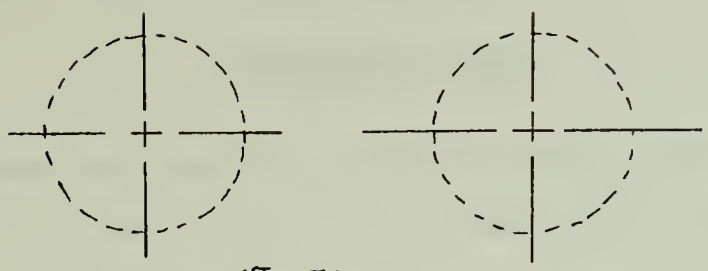

1ST TOP
IMAGE SYSTEM

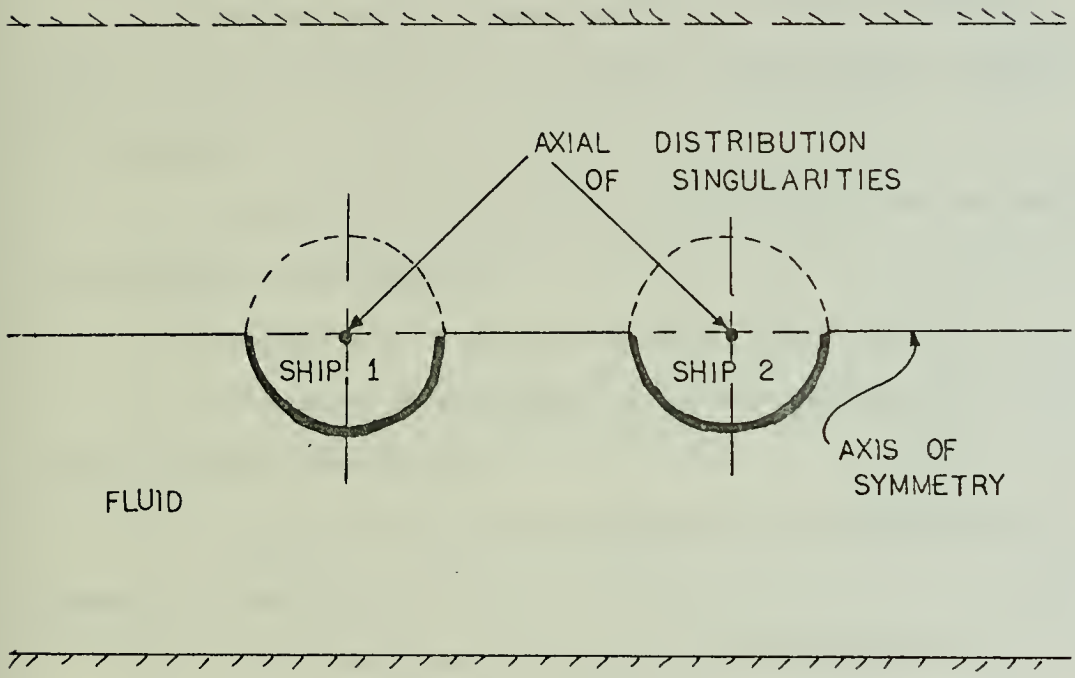

1ST BOTTOM
IMAGE SYSTEM

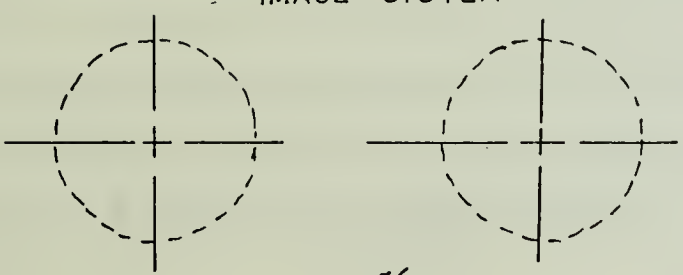

CHAPTER V.

RECOMMENDATIONS

The work accomplished in the thesis points out the need for continued study of the interaction between ships. The following list indicates possible areas for future investigation.

1. Perform model experiments to obtain data to verify Taylor's results, including shallow water effects as described.

2. Include remaining force terms in order to calculate for unsteady ship motions.

3. Incorporate program in trajectory model.

4. Determine stable positions alongside, and test with operating experience.

5. Simulate refueling maneuvers and compare with operator experience.

6. As a final test, attempt to reconstruct published collisions involving ship interactions.

7. Investigate feasibility of extending the theoretical model to include free surface condition by distributing singularities as used by Havelock and developing the required theorems to evaluate the interaction forces as accomplished by R. D. Zucker for vortex sheets.

BIBLIOGRAPHY

1. G. K. Batchelor, An Introduction to Fluid Dynamics, Cambridge University Press, Cambridge, England, 1967.

2. C. N. Calvano, "An Investigation of the Stability of a System of Two Ships Employing Automatic Control While on Parallel Courses in Close Proximity", M.I.T. Thesis, 1970.

3. W. E. Cummins, "The Forces and Moments Acting on a Body Moving in an Arbitrary Potential Stream", David Taylor Model Basin. Report No. 780, Washington, D. C., 1953.

4. R. S. Garthune, et. al., "The Performance of Model Ships in Restricted Channels in Relation to the Design of a Ship Canal", David Taylor Model Basin Report No. 601, Washington, D. C., 1948.

5. R. W. L. Gawn, "The Admiralty Experiment Works, Haslar", Quarterly Transactions of the Institute of Naval Architects, Vol. 97, No. 1, London, England, January, 1955.

6. M. Gertler, "A Reanalysis of the Original Test Data For the Taylor Standard Series", David Taylor Model Basin Report No. 806, Washington, D. C., March, 1954.

7. T. H. Havelock, "The Vertical Force on a Cylinder Submerged in a Uniform Stream", The Collected Papers of Sir Thomas Havelock on Hydrodynamics, Edited by C. Wigley, Office of Naval Research, Department of the Navy, ONR/ACR-103, 1963, pp. 297-303.

8. _____, Discussion to "Interaction Between Ships", by A. M. Robb, Transactions of the Institute of Naval Architects, Vol. 91, London, England, 1949, pp. 336-337.

9. Sir H. Lamb, Hydrodynamics, 6th Edition, Dover Publications, New York, New York, 1932.

10. H. T. Larson and L. M. Tichvinsky, "Replenishment at Sea; Experiments and Comments", University of California Institute of Engineering Research Report No. 154-1, Berkeley, California, June 1, 1960.

11. J. N. Newman, "The Force and Moment on a Slender Body of Revolution Moving Near a Wall", David Taylor Model Basin Report No. 2127, Washington, D. C., 1965.

12. R. N. Newton, "Some Notes on Interaction Effects Between Ships Close Aboard in Deep Water", First Symposium on Ship Maneuverability, David Taylor Model Basin Report No. 1461, Washington, D. C., October, 1960, pp. 1-24.

13. L. Prandtl and O. G. Tietjens, Fundamentals of Hydro and Aero Mechanics, McGraw Hill Book Company, Inc., New York, New York, 1934.

14. B. L. Silverstein, "Linearized Theory of the Interaction of Ships", University of California Institute of Engineering Research Report 82-3, Berkeley, California, May 15, 1957.

15. V. L. Streeter, Fluid Dynamics, McGraw-Hill Book Company, Inc., New York, New York, 1948.

16. D. W. Taylor, "Some Model Experiments on Suction of Vessels", Transaction of the Society of Naval Architects and Marine Engineers, Vol. 17, 1909, pp. 2-22.

17. R. D. Zucker, "Lagally's Theorem and the Lifting Body Problem", Journal of Ship Research, Vol. 14, June, 1970, pp. 135-141.

APPENDICES

APPENDIX A

SSAC (I,J) = Nondimensional sectional area at Station J of Ship I

SAC (I,J) = Sectional area at Station J of Ship I

DSAC (I,J) = Derivative of sectional area at Station J of Ship I

DISPL(I) = Displacement of Ship I (Not used)

LENGT(I) = Length of Ship I

BEAM (I) = Beam of Ship I

VELOC (I) = Velocity (retilinear) of Ship I

CP (I) = Prismatic coefficient of Ship I

CM (I) = Midship coefficent of Ship I

DIST (I) = Distance from midship where R. O. singularities are placed to generate Ship I

S (I,J) = Initial (no interaction) source strength at position J on the axis of Ship I

SM (I,J) = Source strength at position J on the axis of Ship I

SD (I,J) = Dipole strength at position J on the axis of Ship I

NN (I) = Number of stations used to input nondimensional sectional area curve and to perform calculations

KK (I) = Index for Ship I to indicate model used to calculate forces (not used)

X (I) = X position of Ship I in the fluid

Y (I) = Y position of Ship I in the fluid

CI (I) = Heading angle of Ship I in the fluid

PI = The constant

RON = Fluid density

M = Index (not used)

MM = Index (not used)

N = Number of ships interacting
(Program can handle up to 5 with space allocation)

XF1(J) = Component of force in the X direction at Station J

YF1(J) = Component of force in the Y direction at Station J

RF1(J) = Moment at Station J on Ship I

XF2 = Component of force in the X direction of Ship 2

J = Index for indicating position along Ship I

L = Index for indicating position along Ship K

X1(J) = Longitudinal distance to Station J on Ship I

Y1(L) = Longitudinal distance to Station L on Ship K

I = Index to indicate first ship of the pair for force calculation

K = Index to indicate second ship of the pair for force calculation

AFX(I) = Total force on Ship (I) in X direction (Output on non-dimensionalized ED-form)

AFY(I) = Total force on Ship (I) in Y direction

AM(I) = Total moment on Ship I

ACM(I) = Total non-dimensionalized moment for Ship I

QR (I,J) = Total flow at Position J of Ship I (not used)

QA (I,J) = Total axial flow at Position J of Ship I

QN (I,J) = Total transverse flow at Position J of Ship I

DQA (I,J) = Total axial contribution of flow gradient at location J of Ship I

DQN (I,J) = Total transverse contribution of flow gradient at Location J of Ship I

QAZ (L) = Axial flow contribution at J on Ship I due to singularity at L on Ship K

QNZ (L) = Transverse flow contribution

DGNZ (J) = Transverse gradient contribution

QRZ (J) = Flow contribution

DQAZ (J) = Axial gradient contribution

DXI (J) = Station spacing on Ship I between Station J and J+1

DXK (L) = Station spacing on Ship K between L and L+1

AEX (I) = Focal distance of ellipse measured from midship position

APPENDIX B

Derivation of Axis System and Transformations and Potential derivatives

MOVING AXIS SYSTEM

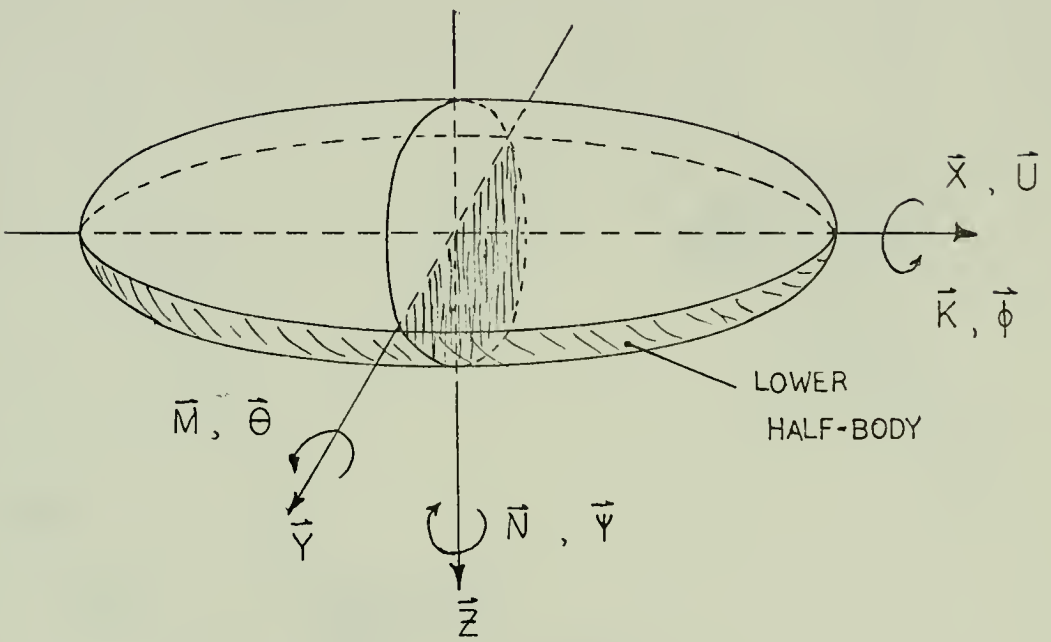

DEFINITION OF AXIS SYSTEMS

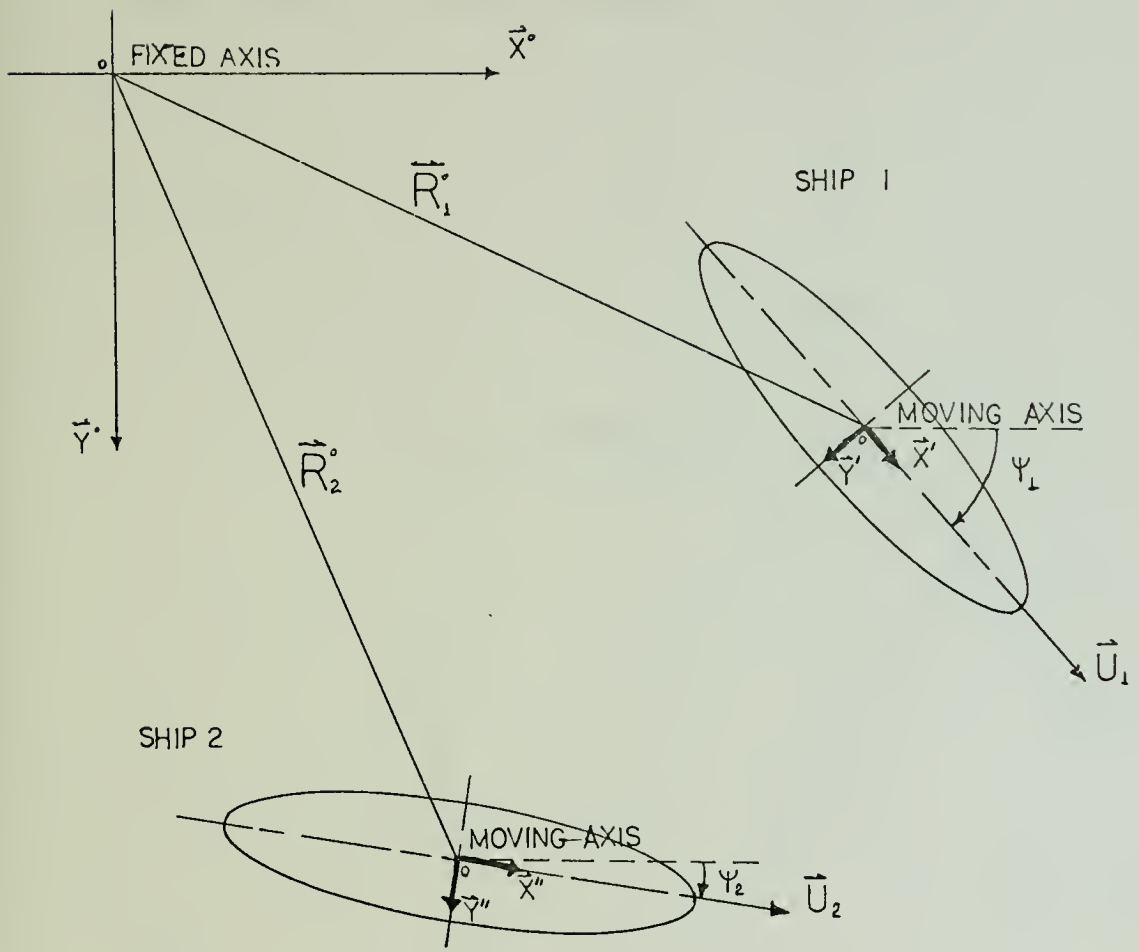

CONVENTION FOR DETERMING · RELATIVE DISTANCES BETWEEN SINGULARITIES IN THE FORCE CALCULATIONS OF SHIP 1

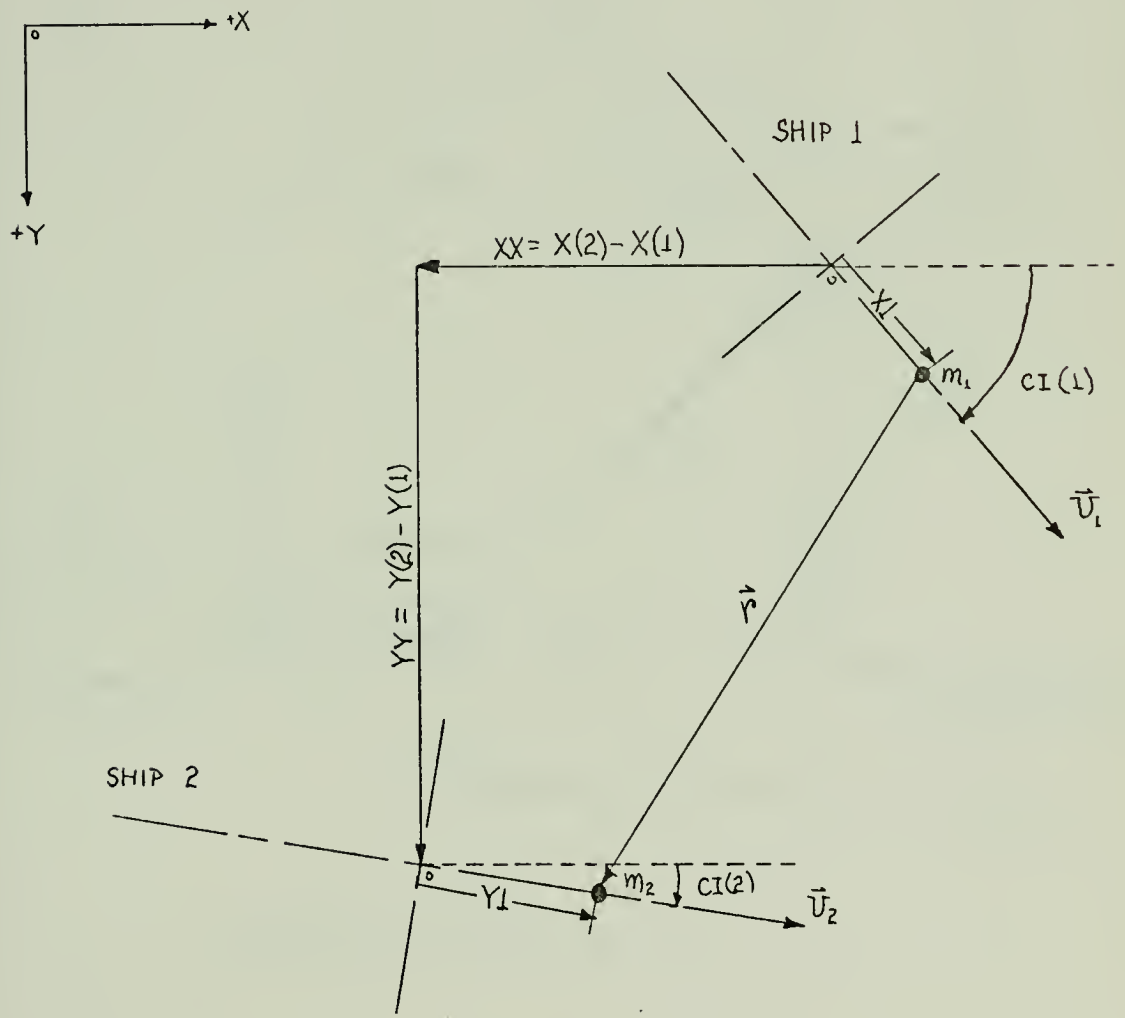

FORCE ON SHIP 1 DUE TO SINGULARITIES M_1 AND M_2

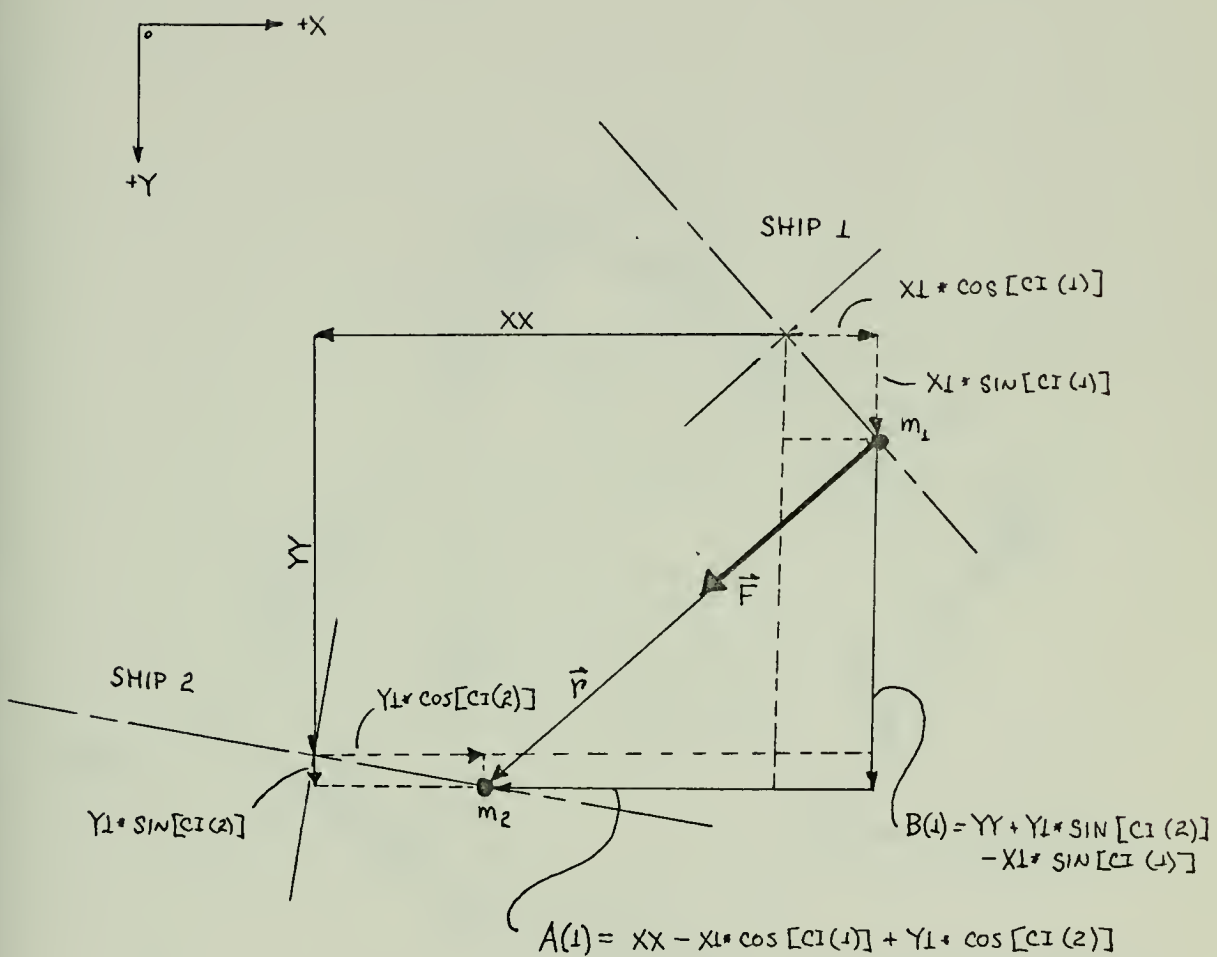

$$\vec{F} = \left(4\pi\rho m_1 m_2 / r^2\right)\hat{r}$$

RESOLUTION OF FORCE ON SHIP 1 INTO AXIAL AND NORMAL COMPONENTS

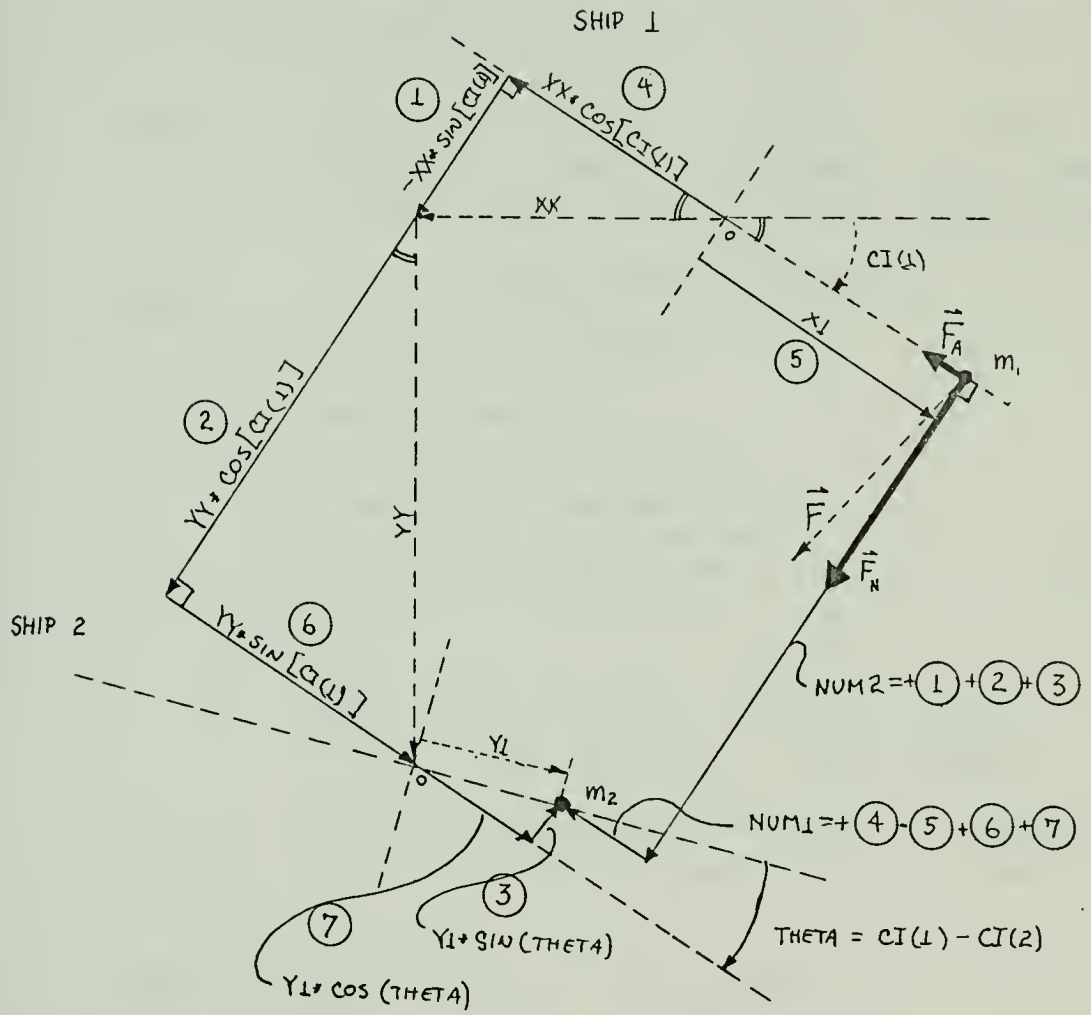

$$\vec{F}_{AXIAL} = |\vec{F}| * NUM1/r$$

$$\vec{F}_{NORMAL} = |\vec{F}| * NUM2/r$$

CALCULATION OF FORCES BETWEEN BODIES USING STEADY FORCE TERMS DERIVED BY H.E. CUMMINS.

* THE SINGULARITY DISTRIBUTIONS ARE DEFINED IN TERMS OF THE SHIP COORDINATES.

GIVEN: POSITION ① IN SHIP K AT WHICH IS LOCATED A SOURCE OF STRENGTH $m_{k,1}$ AND A DOUBLET OF MOMENT $\mu_{k,1}$.

FIND: VARIOUS DERIVATIVES OF POTENTIAL AT POSITION ② IN SHIP I. THESE DERIVATIVES ARE IN TERMS OF THE VARIABLES DESCRIBING THE AXIS SYSTEM OF SHIP I

DEFINE:

$$\textcircled{1}\quad \Phi = \underbrace{U_K}_{\text{due to uniform flow}} + \overbrace{\frac{m}{r} + \frac{\mu \cos\theta}{r^2}}^{\text{due to internal singularities}}$$

AS THE VELOCITY POTENTIAL. THE CONTRIBUTION OF THE UNIFORM FLOW IS EASILY CALCULATED AND WILL NOT BE EVALUATED HERE.

$$\textcircled{2}\quad \Phi'_{TOTAL} = \underbrace{\Phi'}_{\text{DUE TO FIRST ORDER SINGULARITY}} + \underbrace{\Phi'}_{\text{DUE TO SECOND ORDER SINGULARITY}}$$

WHERE: $'$ INDICATES THAT THE POTENTIAL IS DEFINED IN TERMS OF THE AXIS SYSTEM OF SHIP K

THEN:

$$\Phi'_{TOTAL} = \frac{m_{k,1}}{r_1'} + \frac{\mu_{k,1}\cos(\theta')}{(r_1')^2}$$

WHERE: r_1' DEFINES THE DISTANCE FROM POSITION ① IN SHIP K

AND: $r_1' = \left((X_1')^2 + (Y_1')^2\right)^{1/2}$

$\cos(\theta') = \frac{Y_1'}{r_1'}$ {NOTE THAT DIPOLES ARE SITUATED IN THE $\pm Y$ DIRECTION

AT SOME OTHER POSITION, I.E. (2) ON SHIP I

DEFINE: R_{12}' AS THE VECTOR FROM POINT (1) TO POINT (2) DEFINED IN TERMS OF THE AXIS SYSTEM OF SHIP K.

THEN: $\tilde{\Phi}_{TOTAL}'(2) = \frac{m_{K,1}}{R_{12}'} + \frac{\mu_{K,1} Y_{12}'}{(R_{12}')^3}$

WHERE: $R_{12}' = \left((X_{12}')^2 + (Y_{12}')^2\right)^{1/2}$

LET $\mathcal{H}$ BE THE TRANSFORMATION FROM THE SHIP K TO THE SHIP I MOVING AXIS SYSTEM.

THEN: $\tilde{\Phi}_{TOTAL}'' = \mathcal{H}\, \tilde{\Phi}_{TOTAL}'$

WHERE: " INDICATES THAT THE POTENTIAL IS DEFINED IN TERMS OF THE AXIS SYSTEM OF SHIP I

THIS IS EQUIVALENT TO SUBSTITUTING VARIABLES DEFINED:

$$\begin{bmatrix} X_1'' \\ Y_1'' \end{bmatrix} = \mathcal{H} \begin{bmatrix} X_1' \\ Y_1' \end{bmatrix}$$

WHERE: THE SUBSCRIPT "1" REMINDS US THAT THE ORIGIN OF THE AXIS SYSTEM IS AT POSITION (1).

THE DETERMINATION OF THE EXPRESSIONS FOR X_1'' AND Y_1'' FOLLOW. THE SUPERSCRIPT '0' INDICATES THAT THE VARIABLE IS DEFINED IN A FIXED REFERANCE AXIS SYSTEM.

LET:

$$T_K \triangleq \begin{bmatrix} \cos\Psi_K & \sin\Psi_K \\ -\sin\Psi_K & \cos\Psi_K \end{bmatrix}$$

$$T_I \triangleq \begin{bmatrix} \cos\Psi_I & \sin\Psi_I \\ -\sin\Psi_I & \cos\Psi_I \end{bmatrix}$$

THEN:

$$T_K^{-1} = \begin{bmatrix} \cos\Psi_K & -\sin\Psi_K \\ \sin\Psi_K & \cos\Psi_K \end{bmatrix}$$

$$T_I^{-1} = \begin{bmatrix} \cos\Psi_I & -\sin\Psi_I \\ \sin\Psi_I & \cos\Psi_I \end{bmatrix}$$

WHERE:

$\Psi_K \triangleq$ THE HEADING ANGLE OF SHIP K BASED UPON A FIXED AXIS SYSTEM

$\Psi_I \triangleq$ THE HEADING ANGLE OF SHIP I BASED UPON A FIXED AXIS SYSTEM

DEFINING:

$$\bar{r}_1' \triangleq \begin{bmatrix} X_1 \\ Y_1 \end{bmatrix}$$

$$\bar{r}_1' = T_K [\bar{r}_1^\circ]$$

$$\bar{r}_1'' = T_I [\bar{r}_1^\circ]$$

$$\begin{bmatrix} X_1'' \\ Y_1'' \end{bmatrix} = \bar{r}_1'' = T_I [\bar{r}_1^\circ] = T_I [T_K^{-1} [\bar{r}_1']] = T_I T_K^{-1} \begin{bmatrix} X_1' \\ Y_1' \end{bmatrix}$$

OR

$$\begin{bmatrix} X_1' \\ Y_1' \end{bmatrix} = T_K T_I^{-1} \begin{bmatrix} X_1'' \\ Y_1'' \end{bmatrix}$$

EXPANDING :

$$X_1' = X_1'' \cos(\Psi_K - \Psi_I) + Y_1'' \sin(\Psi_K - \Psi_I)$$

$$Y_1' = -X_1'' \sin(\Psi_K - \Psi_I) + Y_1'' \cos(\Psi_K - \Psi_I)$$

$$(r_1')^2 = (r_1'')^2$$

SUBSTITUTING BACK INTO THE POTENTIAL DEFINED IN TERMS OF THE MOVING AXIS SYSTEM OF SHIP K, THE SAME POTENTIAL FIELD IS DEFINED IN TERMS OF THE MOVING AXIS SYSTEM OF SHIP I.

$$\Phi''_{TOTAL} = \frac{m_{k,1}}{r_1''} + \frac{\mu_{k,1}\left[-X_1'' \sin(\Psi_k - \Psi_I) + Y_1'' \cos(\Psi_k - \Psi_I)\right]}{(r_1'')^3}$$

r_1'' IS STILL MEASURED FROM POSITION ① ON SHIP K, ALSO WE WILL DROP THE SUBSCRIPTS ON THE SINGULARITIES.

PROCEEDING TO THE DETERMINATION OF DERIVATIVES —

THE EVALUATION OF EACH DERIVATIVE WILL BE AT POSITION ② ON SHIP I. WE NEED THE QUANTITY $\bar{R}_{12}'' \triangleq$ THE VECTOR FROM POINT ① TO POINT ② IN TERMS OF THE MOVING AXIS SYSTEM OF SHIP I.

LET: $X^{\circ}(I)$ ≡ DEFINE THE DISTANCE TO THE ORIGIN OF THE MOVING AXIS SYSTEM OF SHIP I FROM SOME REFERENCE POSITION

$X^{\circ}(K)$ ≡ THE SAME FOR SHIP K

$XI''(L)$ ≡ DEFINES THE DISTANCE ALONG THE AXIS OF SHIP I TO POSITION ②

$YI'(J)$ ≡ DEFINES THE DISTANCE ALONG THE AXIS OF SHIP K TO POSITION ①

$$\bar{R}^{\circ}_{12} = \text{POSITION OF ②} - \text{POSITION OF ①}$$

$$= \overbrace{\begin{bmatrix} X^{\circ}(I) \\ Y^{\circ}(I) \end{bmatrix} + T_I^{-1} \begin{bmatrix} XI''(L) \\ 0 \end{bmatrix}} - \overbrace{\left(\begin{bmatrix} X^{\circ}(K) \\ Y^{\circ}(K) \end{bmatrix} + T_K^{-1} \begin{bmatrix} YI''(J) \\ 0 \end{bmatrix} \right)}$$

$$= \begin{bmatrix} X^{\circ}(I) \\ Y^{\circ}(I) \end{bmatrix} + \begin{bmatrix} XI''(L)\cos\psi_I \\ XI''(L)\sin\psi_I \end{bmatrix} - \left(\begin{bmatrix} X^{\circ}(K) \\ Y^{\circ}(K) \end{bmatrix} + \begin{bmatrix} YI''(J)\cos\psi_K \\ YI''(J)\sin\psi_K \end{bmatrix} \right)$$

$$\bar{R}^{\circ}_{12} = \begin{bmatrix} X^{\circ}(I) - X^{\circ}(K) + XI''(L)\cos\psi_I - YI''(J)\cos\psi_K \\ Y^{\circ}(I) - Y^{\circ}(K) + XI''(L)\sin\psi_I - YI''(J)\sin\psi_K \end{bmatrix}$$

$$\bar{R}''_{12} = T_I \left[\bar{R}^{\circ}_{12} \right] = \begin{bmatrix} \cos\psi_I & \sin\psi_I \\ -\sin\psi_I & \cos\psi_I \end{bmatrix} \begin{bmatrix} \quad \end{bmatrix}$$

LET: $\psi_K - \psi_I$ = THETA

$X^{\circ}(K) - X^{\circ}(I) = XX$

$Y^{\circ}(K) - Y^{\circ}(I) = YY$

AT POSITION ③ ON SHIP I THE DERIVATIVES WILL BE EVALUATED AT X''_{12} , Y''_{12} WHERE

$$X''_{12} = -XX\cos\Psi_J - YY\sin\Psi_I - Y_{I(J)}\cos(THETA) + X_{I(L)}$$

$$Y''_{12} = +XX\sin\Psi_I - YY\cos\Psi_I - Y_{I(J)}\sin(THETA)$$

BY DEFINITION :

⊙ THE AXIAL FLOW ALONG SHIP I AT ② $_1$ DUE TO SINGULARITIES ON SHIP K =

$$QA2(②) = -\frac{\partial\Phi''}{\partial x''}\bigg|_{②}$$

$$\frac{\partial\Phi''}{\partial x''} = \frac{-m\,x''}{(r''_1)^3} - \frac{3\mu\,x''\left(-X''\sin(THETA) + Y''\cos(THETA)\right)}{(r''_1)^5}$$

$$- \frac{\mu\sin(THETA)}{(r''_1)^3}$$

EVALUATING AT ②

$$QA2(②) = -\frac{\partial\Phi''}{\partial x''} = \frac{m\,X''_{12}}{(\bar{R}''_{12})^3} + \frac{3\mu\,X''_{12}\left(-X''_{12}\sin(THETA) + Y''_{12}\cos(THETA)\right)}{(\bar{R}''_{12})^5}$$

$$+ \frac{\mu\sin(THETA)}{(\bar{R}''_{12})^3}$$

⊙ THE NORMAL (CROSS) FLOW =

$$QN2(②) = -\left.\frac{\partial \Phi''}{\partial Y''}\right|_{②}$$

$$QN2(②) = \frac{+m\,Y''_{12}}{(R''_{12})^3} + \frac{3\mu\,Y''_{12}\left(-X''_{12}\sin(THETA)+Y''_{12}\cos(THETA)\right)}{(R''_{12})^5}$$

$$-\frac{\mu\cos(THETA)}{(R''_{12})^3}$$

⊙ THE EVALUATION OF FORCE CONTRIBUTION OF DOUBLETS REQUIRES THE EVALUATION OF

$$\left.\frac{\partial^2 \Phi''}{(\partial Y'')^2}\right|_{②} \text{ & } \left.\frac{\partial^2 \Phi''}{\partial X''\partial Y''}\right|_{②}$$

$$\left.\frac{\partial^2 \Phi}{\partial x''\partial Y''}\right|_{②} = \frac{m\,Y''_{12}X''_{12}}{(R''_{12})^5} + \frac{15\mu\,Y''_{12}X''_{12}\left(-X''_{12}\sin(THETA)+Y''_{12}\cos(THETA)\right)}{(R''_{12})^7}$$

$$+\frac{3\mu Y''_{12}\sin(THETA)}{(R''_{12})^5} - \frac{3\mu X''_{12}\cos(THETA)}{(R''_{12})^5}$$

$$\left.\frac{\partial^2 \bar{\Phi}''}{(\partial Y'')^2}\right|_{②} = \frac{-m}{(R''_{12})^3} + \frac{3m\,Y''_{12}}{(R''_{12})^5} - \frac{3\mu\,Y''_{12}\cos(\text{THETA})}{(R''_{12})^5}$$

$$- \frac{3\mu\left(-X''_{12}\sin(\text{THETA}) + Y''_{12}\cos(\text{THETA})\right)}{(R''_{12})^5}$$

$$+ \frac{15\,\mu\,(Y''_{12})^2\left(-X''_{12}\sin(\text{THETA}) + Y''_{12}\cos(\text{THETA})\right)}{(R''_{12})^7}$$

APPENDIX C

DERIVATION OF THE 3-DIMENSIONAL SOURCE SINGULARITY DISTRIBUTION FOR A SLENDER BODY.

A CONTINUOUS AXIAL DISTRIBUTION OF SINGULARITIES WHICH REPRESENTS A BODY MOVING IN A UNIFORM STREAM GIVES THE POTENTIAL –

$$\Phi(x) = -U(x) + \int_a^b \frac{m(\xi)}{\sqrt{(x-\xi)^2+Y^2+Z^2}}\, d\xi$$

FIND: $m(\xi)$ FOR A SLENDER BODY

THE FLOW CONDITION AT THE SURFACE OF THE BODY REQUIRES NO FLOW ACROSS THE RIGID BOUNDARY. FOR A SLENDER BODY THE NORMAL DIRECTION IS ASSUMED CLOSE TO THE RADIAL AND THE FOLLOWING EQUATION HOLDS,

$$v_{RADIAL}(x)\Big|_{BODY} = 0$$

WHERE: DUE TO INTERNAL SINGULARITIES

$$v_r(x)\Big|_{BODY} = -\frac{\partial \Phi(x)}{\partial r}\Big|_{BODY} = -\left[0 + \int \frac{\partial}{\partial r}\frac{m(\xi)}{\sqrt{(x-\xi)^2+r^2}}\, d\xi\Big|_{r=R}\right]$$

WHERE $r = (Y^2+Z^2)^{1/2}$

TAKING THE DERIVATIVE:

$$-\left.\frac{\partial \bar{\Phi}(x)}{\partial r}\right|_{r=R} = -\int_a^b \frac{1}{2}\frac{m(\xi)\,2R}{\left((x-\xi)^2+R^2\right)^{3/2}}\,d\xi$$

$$= +\int_a^b \left(\frac{1}{R^3}\right)\frac{m(\xi)\,R}{\left[\left(\frac{\xi-x}{R}\right)^2+1\right]^{3/2}}\,d\xi$$

LET $\frac{\xi-x}{R} = A \qquad d\left(\frac{\xi-x}{R}\right) = \frac{1}{R}\,d\xi$

THEN:

$$-\left.\frac{\partial \bar{I}(x)}{\partial r}\right|_{r=R} = \frac{1}{R}\int_a^b \frac{m(\xi)\; d\left(\frac{\xi-x}{R}\right)}{\left(\left(\frac{\xi-x}{R}\right)^2+1\right)^{3/2}}$$

$$\approx \frac{m(x)}{R}\int_{-\infty}^{\infty}\frac{dA}{(A^2+1)^{3/2}} = \frac{2\,m(x)}{R}$$

WHERE: DUE TO THE EXTERNAL FLOW -

$$v_{\text{RADIAL}}\Big|_{\text{BODY}} = U\frac{dR}{dx} = \frac{2m(x)}{R}$$

THEN: $$m(x) = \frac{UR}{2}\frac{dR}{dx} = \frac{U\,S'(x)}{4\pi}$$

WHERE: $S'(x)$ IS THE DERIVATIVE OF THE SECTIONAL AREA CURVE WITH RESPECT TO x EVALUATED AT x

DERIVATION OF A 3-DIMENSIONAL DOUBLET DISTRIBUTION WHICH REPRESENTS A INFINATE CYLENDER IN A UNIFORM CROSS FLOW.

$$\Phi(x) = \int_{a=-\infty}^{b=\infty} \frac{\mu(\xi)\, Y}{r^3}\, d\xi$$

THE BOUNDARY CONDITION IS SUCH THAT

$$-\frac{\partial \Phi}{\partial Y}\bigg|_{\substack{Z=0 \\ R=\text{BOUNDARY}}} = V_{\text{CROSS FLOW}}$$

THUS:

$$V = -\frac{\partial}{\partial Y}\left[\int_{x=-\infty}^{b=\infty} \frac{\mu(\xi)\, Y\, d\xi}{\left((x-\xi)^2 + Y^2 + Z^2\right)^{3/2}}\right]_{\substack{Y=R \\ Z=0 \\ R=\text{BOUNDARY } X}}$$

$$= -\frac{2\mu(x)}{R^2} + \frac{6\mu(x)}{R^2}\left[\lim_{\substack{a\to\infty \\ b\to\infty}} \int_a^b \frac{dB}{(B^2+1)^{5/2}}\right]$$

WHERE $B = \overset{X}{\mu}\left(\frac{\xi - x}{R}\right)$

$$V = -\frac{2\mu(x)}{R^2} + \frac{6\mu(x)}{R^2}\left[\frac{B}{(B^2+1)^{1/2}} - \frac{1}{3}\frac{B^3}{(B^2+1)^{3/2}}\right]_0^\infty$$

$$= -\frac{2\mu(x)}{R^2} + \frac{6\mu(x)}{R^2}\left(\frac{2}{3}\right)$$

OR

$$V = \frac{2\mu(x)}{R^2}$$

$$\mu(x) = \frac{VR^2}{2} = \frac{2V\pi R^2}{4\pi} = \frac{2V\,S(x)}{4\pi}$$

WHERE: $S(x)$ = SECTIONAL AREA CURVE EVALUATED AT X

APPENDIX D

SINGULARITY DISTRIBUTIONS

The following graphs depict some of the representative singularity distributions.

Model of an ellipse with L/B=6, L= 600 ft., V= 10 kts.

ELLIPSOID APPROXIMATION (NO CROSS FLOW)

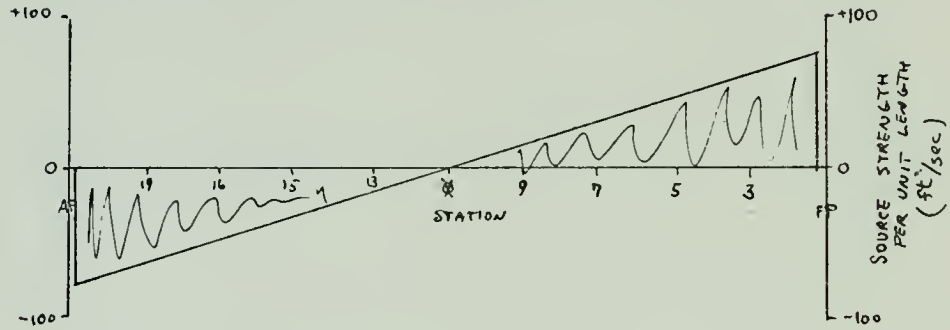

RANKINE OVOID APPROXIMATION (NO CROSS FLOW)

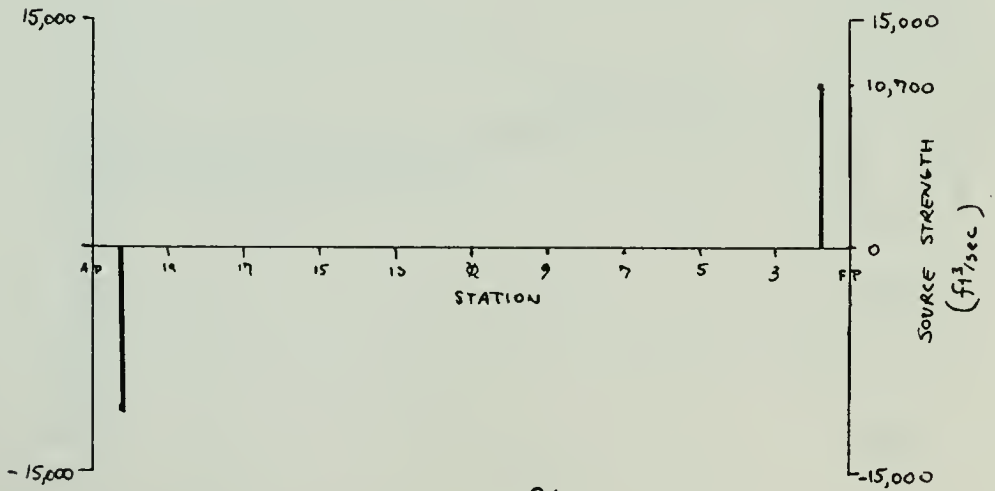

The modified ellipsoid has three singularity distri-

when placed moving parallel to a wall with

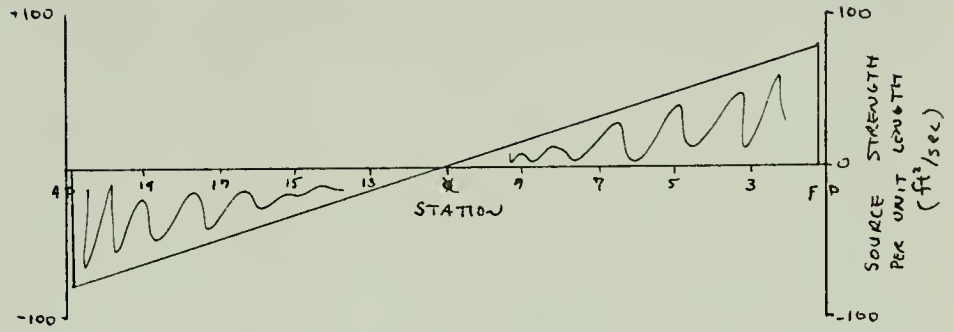

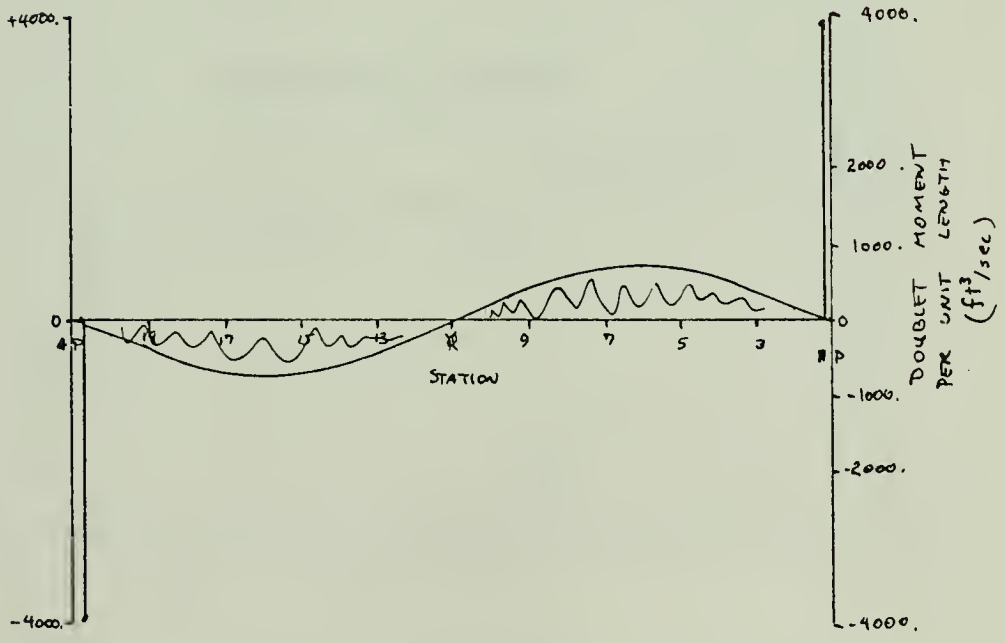

The distributions used to model the Taylor full ship results are as follows. The situation when the models are abeam with a 3.9 ft. separation is represented (end corrections included).

SLENDER BODY APPROXIMATION

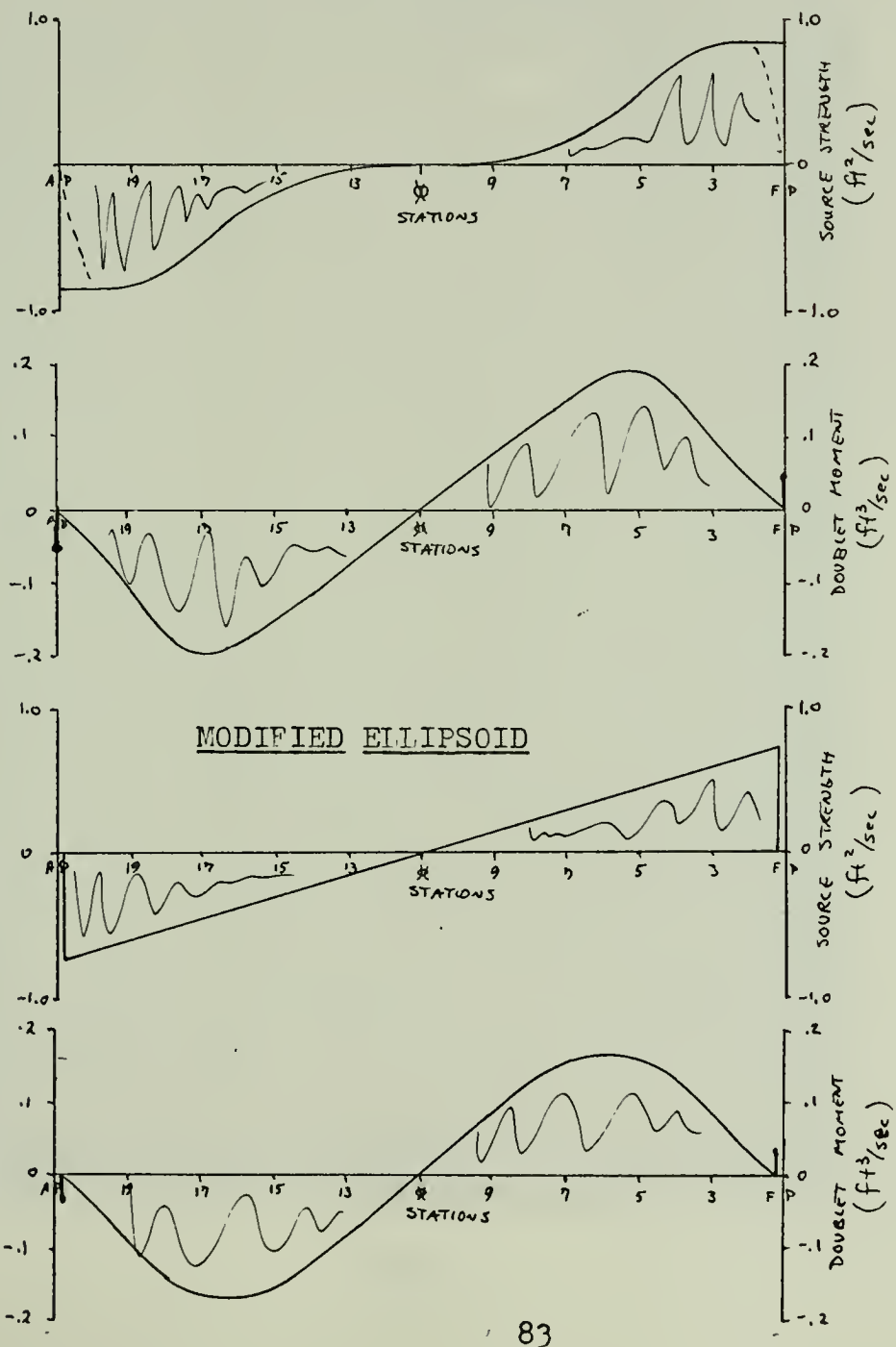

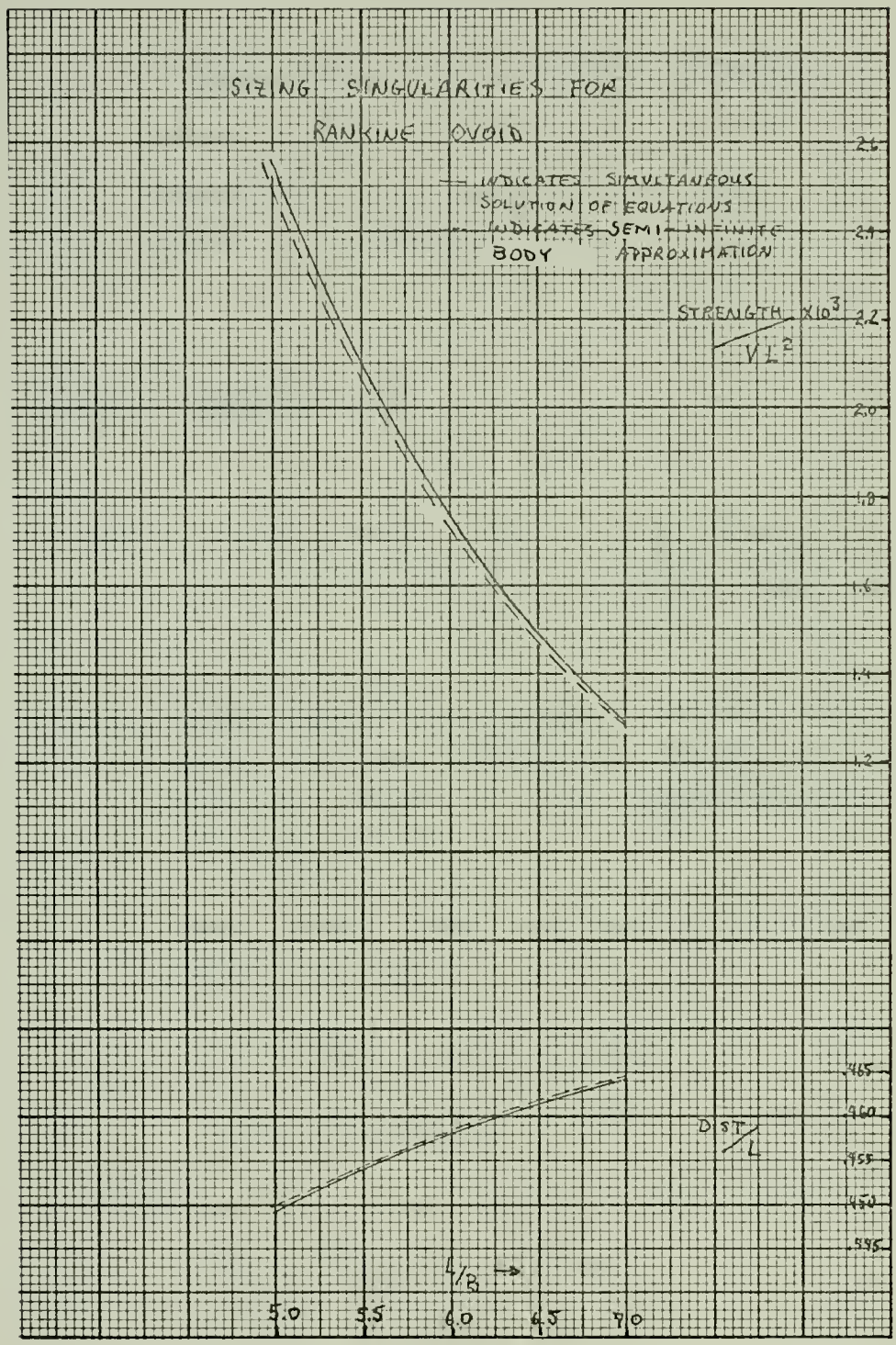
SIZING SINGULARITIES FOR
RANKINE OVOID
— INDICATES SIMULTANEOUS SOLUTION OF EQUATIONS
--- INDICATES SEMI-INFINITE BODY APPROXIMATION
STRENGTH X10^3
V L^2
2.6
2.4
2.2
2.0
1.8
1.6
1.4
1.2
.465
.460
.455
.450
.595
DIST / L
L/B →
5.0
5.5
6.0
6.5
7.0

APPENDIX E

CALCULATION OF POSIBLE ERRORS IN TAYLOR MODEL TEST AND IN THE NEUMERICAL INTEGRATION OF THE FORCE INTEGRALS.

TAYLOR MODEL TESTS

ASSUME FULL MODEL WITH $L = 20.512'$, $B = 3.59'$, $T = .957'$, $C_p = .74$, $C_B = .68$

USING DATA FROM "THE STEERING CHARACTERISTICS OF SHIPS IN CALM WATER AND WAVES", BY H. EDA AND C.L. CRANE, IN THE TRANSACTIONS OF SNAME, 1965, PP 135-179.

THEIR MODEL #70 HAD SIMILAR GEOMETRIC PROPERTIES FROM THE DATA

$$Y'_v = Y_v / \tfrac{1}{2}\rho L T^2 U^2 = -.324$$

$$N'_v = N_v / \tfrac{1}{2}\rho L^2 T^2 U^2 = -.104$$

WHERE v = SLIP VELOCITY

CONVERTING TO THE NON-DIMENSIONAL FORM USED IN THE THEYS-

$$C_{Y_v} = Y_v / \tfrac{1}{2}\rho L^2 U^2 = 1.5 \times 10^{-2}$$

$$C_{N_v} = N_v / \tfrac{1}{2}\rho L^3 U^2 = 4.85 \times 10^{-3}$$

WHERE v = COMPONENT OF FLUID FLOW

* SIGN CHANGE DUE TO CHANGE IN DEFINITION OF "v"

ASSUME A +1° ANGLE DUE TO MISALIGNMENT:

$1^\circ \rightarrow .017$ RADIANS

FOR THE 2.5 KNOT TWO SPEED, THIS INTRODUCES A SLIP VELOCITY OF .07 FT/sec. FOR SMALL ANGLES -

$$Y \sim v\, Y_v = (.07)(Y_v)$$
$$N \sim v\, N_v = (.07)(N_v)$$

$$\frac{N}{\frac{1}{2}\rho U^2 L^3} = (.07)(C_{N_v}) = (.07)(4.85 \times 10^{-3}) = 3.39 \times 10^{-4}$$

$$\frac{Y}{\frac{1}{2}\rho U^2 L^2} = (.07)(C_{Y_v}) = (.07)(1.5 \times 10^{-2}) = 1.05 \times 10^{-3}$$

INTEGRATION:

SIMPSON'S RULE (OVER) ESTIMATES THE INTEGRAL VALUE BY THIS ERROR TERM

$$-\frac{(b-a)}{180} h^4 f^{(4)}(\xi)$$

FOR THE CASE OF AN AXIAL DISTRIBUTION OF SOURCE SINGULARITIES

$$f^{(4)}(\xi) \equiv 0$$

THE COMPUTATIONS WERE ONLY ACCURATE TO 7 SIGNIFICANT FIGURES FOR ALL CASES.

A MEASURE OF THE ERROR WOULD BE

$$-\left(\frac{L}{180}\right)\left(\frac{L}{NL}\right)(.0000001)$$

FOR THE CASE IN NEWMAN'S PROBLEM WHERE $L/B = 60$ EACH INTEGRATION INTRODUCED AN ERROR

$$\epsilon \approx -\left(\frac{6000}{180}\right)\left(\frac{6000}{20}\right)(.0000001)$$

BECAUSE IT WAS NECESSARY TO PERFORM THE INTEGRATION TWICE (DOUBLE INTEGRAL) THE ERROR WOULD BE EQUAL TO ϵ^2

$$\epsilon^2 \approx 1. \times 10^{-6}$$

APPENDIX F

Presentation of Ellipsoid and Rankine Ovoid Results (Compare with original work)

The results are the same except for a scale change. Havelock's scale should be divided by 10, where Silverstien's should be divided by $(4\pi)^2$, or 158.

APPENDIX G

COMPUTATION EFFICIENCY

The programs written without cross flow corrections take only a fraction of a second to evaluate interaction forces for each individual ship position. The slender body model with cross flow corrections takes various times for execution depending on the number of iterations of the flows required. For the samples run, two ships with twenty one stations each, took three seconds for five iterations increased to ten, the time doubled to six seconds for each ship position calculated.

APPENDIX H

Applications Program Series
AP-21 revision 2

MASSACHUSETTS INSTITUTE OF TECHNOLOGY
INFORMATION PROCESSING CENTER

September 28, 1973

NAME: ZEROIN, a double precision FORTRAN IV subroutine to solve a system of simultaneous, nonlinear equations

DESCRIPTION: ZEROIN computes a solution vector $\underline{X}$ of a set of N simultaneous, nonlinear equations:

$$F_1(\underline{X})=0,$$
$$\vdots$$
$$F_n(\underline{X})=0.$$

METHOD: $\underline{X}$ is obtained by an iterative method:

$$\underline{X}^{(k+1)} = \underline{X}^{(k)} + \underline{D}^{(k)}$$

where the vector $\underline{D}^{(k)} = J^{(k)} * \underline{F}(\underline{X}^{(k)})$, with $\underline{F}(\underline{X}^{(k)})$ representing the vector of function values at the point $\underline{X}^{(k)}$ and $J^{(k)}$ representing an approximation to the Jacobian at $\underline{X}^{(k)}$. The following test is used to determine convergence:

$$||\underline{X}^{(k+1)} - \underline{X}^{(k)}||^2 \leq EPS * ||\underline{X}^{(k+1)}||^2$$

where EPS is a user-supplied tolerance. All real arithmetic in ZEROIN is double-precision.

USAGE: The call for ZEROIN is:

```
CALL ZEROIN(N,X,R,EPS,ICV,EVAL,IRITE)
```

Input values are:

N — the order of the system of equations, $2 \leq N \leq 20$.

X — a one-dimensional array initially containing an estimate of the solution vector.

R — an estimate for ||solution vector-$\underline{X}$||

EPS — a tolerance to be used in the test for convergence, usually 0.5E-12.

IRITE — a specification for intermediate printing. If IRITE = 0, ZEROIN does no printing. If IRITE = 1, ZEROIN prints, at each iteration, the current value of R, the current approximation to the solution, the number of times EVAL (below) has been called, and the current function values $\underline{F}(\underline{X})$. The printed output from the final iteration contains, in addition, the output value of ICV.

EVAL — is the name of a user-supplied SUBROUTINE subprogram that evaluates the functions F at each iteration. The call for EVAL is CALL EVAL(X,F) where X is the input to EVAL, and F contains the function values corresponding to X. X and F must be singly-dimensioned, double-precision vectors.

Output values will be:

X — the solution vector.

R — $||\underline{X}^{(k+1)} - \underline{X}^{(k)}||^2 / ||\underline{X}^{(k+1)}||^2$

where $\underline{X}^{(k+1)}$ is the solution vector. When ZEROIN terminates normally, the output value of R will be less than the initial value of EPS. In case of abnormal termination, R can be used to determine what degree of convergence was obtained in the output value of X.

EPS — $||\underline{F}(\underline{X})||^2$ where $\underline{F}(\underline{X})$ is the vector of function values corresponding to the solution vector $\underline{X}$.

ICV — one of the following indications:

ICV = 0 if convergence was obtained, but $||\underline{F}(\underline{X})||^2 > 0.5E-10$

ICV = 1 if convergence was obtained, and $||\underline{F}(\underline{X})||^2 \leq 0.5E-10$

ICV = 2 if convergence was not obtained within M iterations, where M = MIN(10*N,50).

Appropriate declarations are:

```
REAL*8          X(N), R, EPS, EVAL
INTEGER*4       N, ICV, IRITE
EXTERNAL        EVAL
```

CODING CONSIDERATIONS:

1. The input value of R may be chosen to be $||\underline{X}||/10.0$, where $\underline{X}$ is the input vector of estimates, if the solutions are all about the same magnitude.

2. The output value of R can be used to determine degree of convergence in the case ICV=2.

3. ZEROIN is more likely to converge if the equations are scaled so all solutions are of the same magnitude, and if the initial estimates are good. Poor initial estimates may produce divide check interrupts during execution of ZEROIN. For details on the choice of initial estimates, refer to the first reference below.

AVAILABILITY: ZEROIN is available in load module form in the library SYS5.MATHLIB.SUBR and in source form in SYS5.MATHLIB.SOURCE. For further information about the use of these libraries, refer to AP-60 or consult the Programming Assistants in Room 39-219.

CORE REQUIREMENT: On the 370/165 ZEROIN uses 9,730 bytes of core storage (hexadecimal 2602).

REFERENCES:

Mancino, O.G. "Resolution by Iteration of Some Nonlinear Systems," Journal of the Association for Computing Machinery, Vol. 14, No. 2 (April, 1967), pages 341-350.

Robinson, S.M. "Interpolative Solution of Systems of Nonlinear Equations," SIAM Journal on Numerical Analysis, Vol. 3, No. 4 (December, 1966), page 650.

AUTHOR: ZEROIN was written by G.W. Westley, Computing Technology Center, Union Carbide Corporation, Nuclear Division, Oak Ridge, Tennessee.

APPENDIX I

Computer Flow Chart

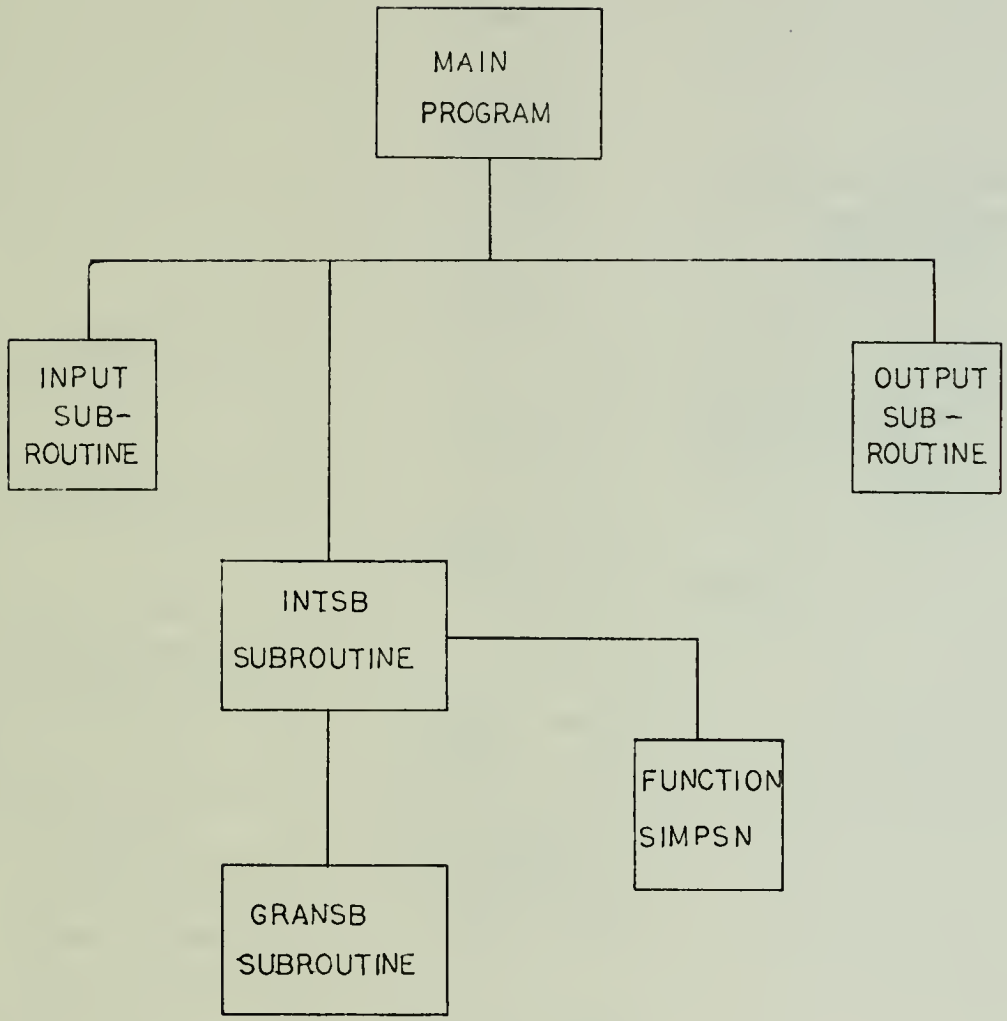

RELATIONSHIP BETWEEN PROGRAMS

MAIN PROGRAM

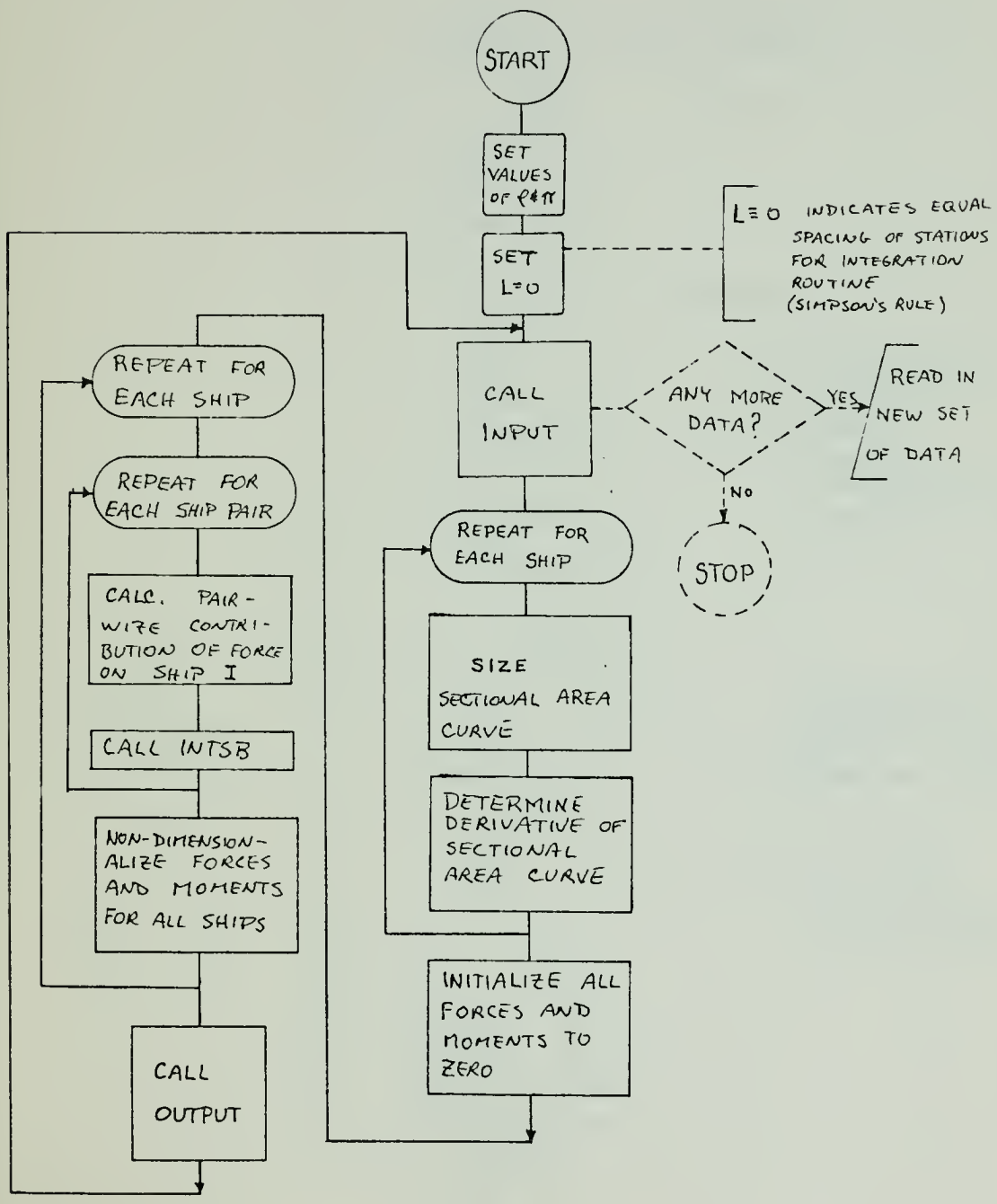

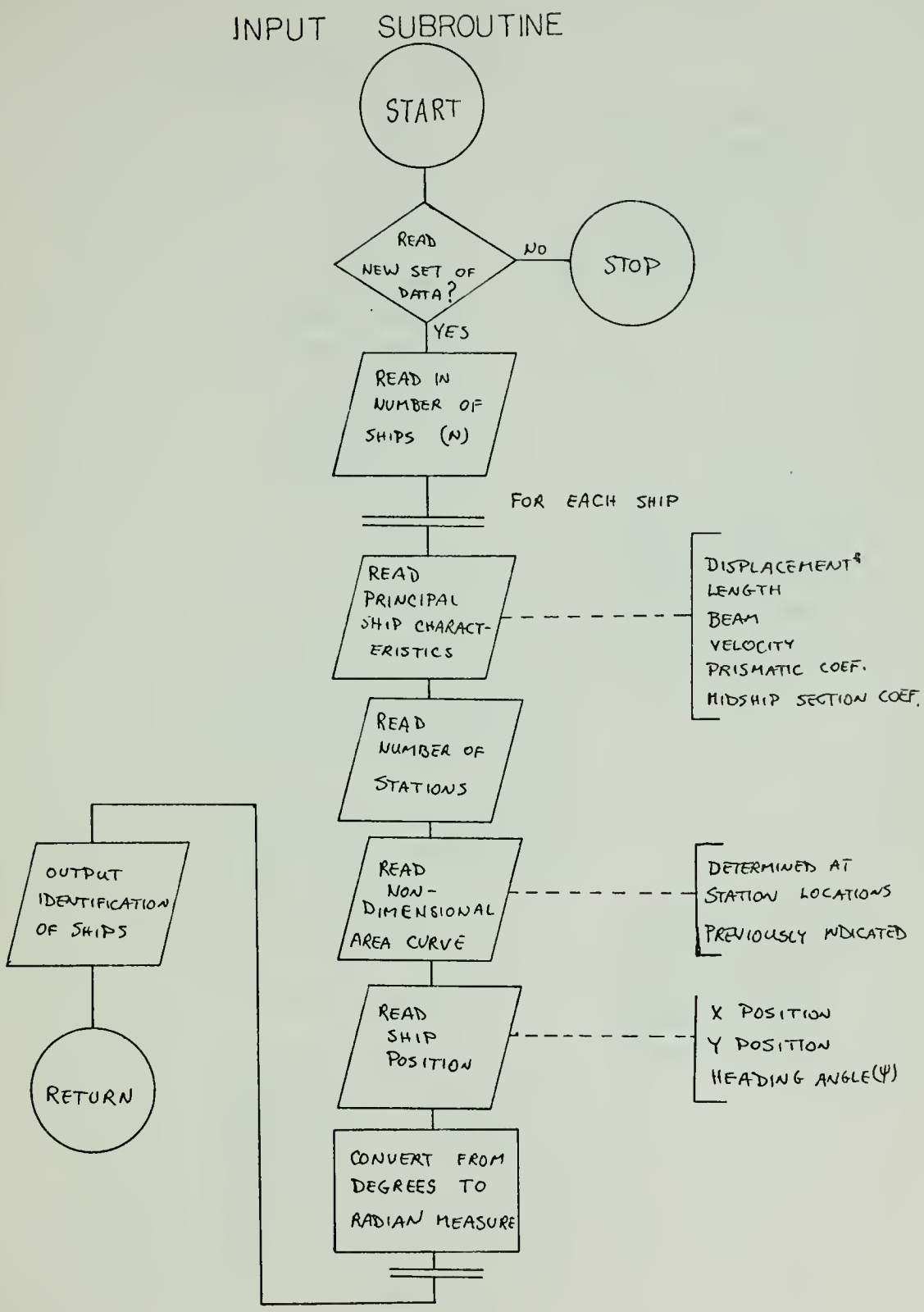
INPUT SUBROUTINE
START
READ NEW SET OF DATA?
NO
STOP
YES
READ IN NUMBER OF SHIPS (N)
FOR EACH SHIP
READ PRINCIPAL SHIP CHARACT-ERISTICS
DISPLACEMENT
LENGTH
BEAM
VELOCITY
PRISMATIC COEF.
MIDSHIP SECTION COEF.
READ NUMBER OF STATIONS
READ NON-DIMENSIONAL AREA CURVE
DETERMINED AT STATION LOCATIONS PREVIOUSLY INDICATED
READ SHIP POSITION
X POSITION
Y POSITION
HEADING ANGLE(Ψ)
CONVERT FROM DEGREES TO RADIAN MEASURE
OUTPUT IDENTIFICATION OF SHIPS
RETURN

SUBROUTINE INTSB

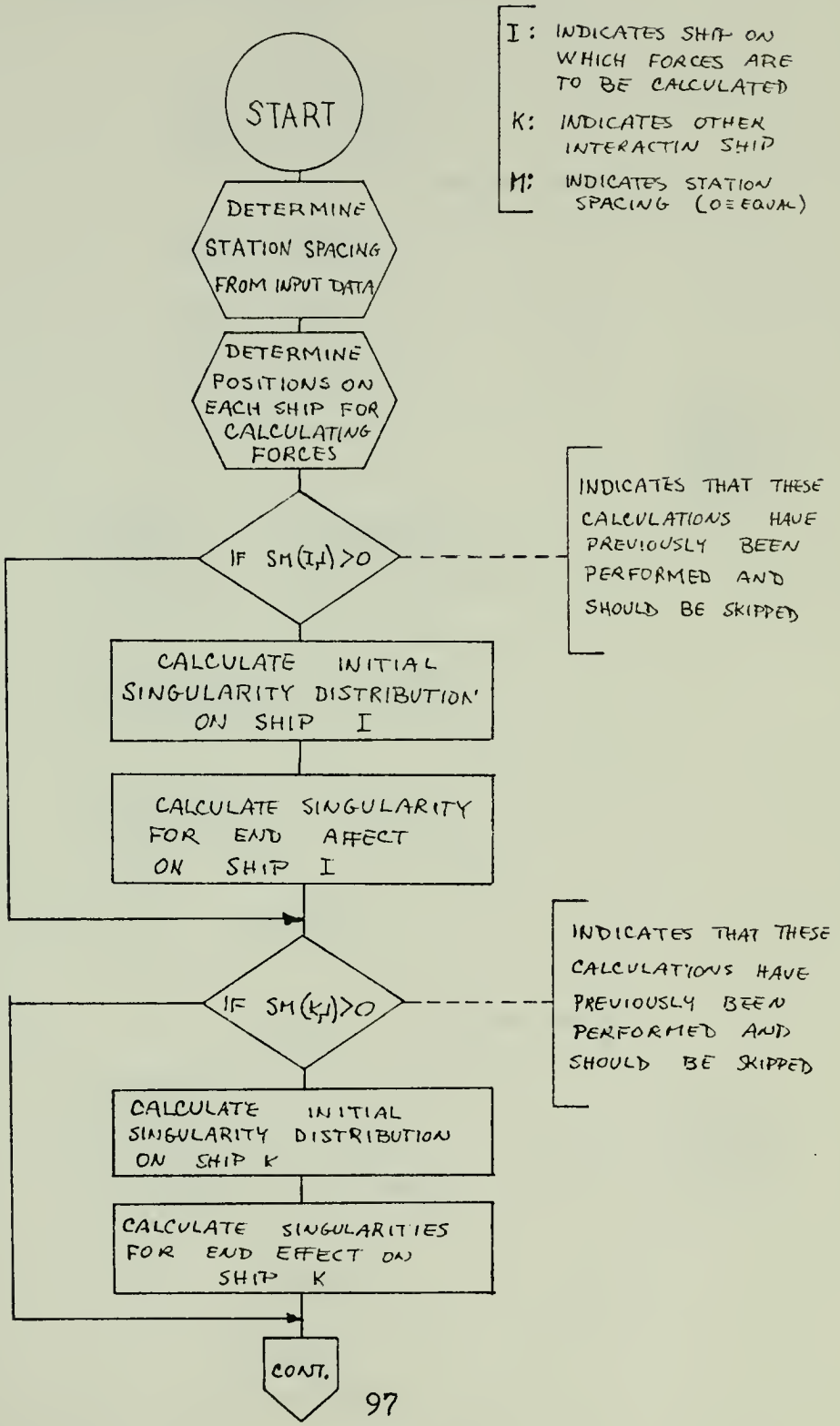

SUBROUTINE INTSB (CONT.)

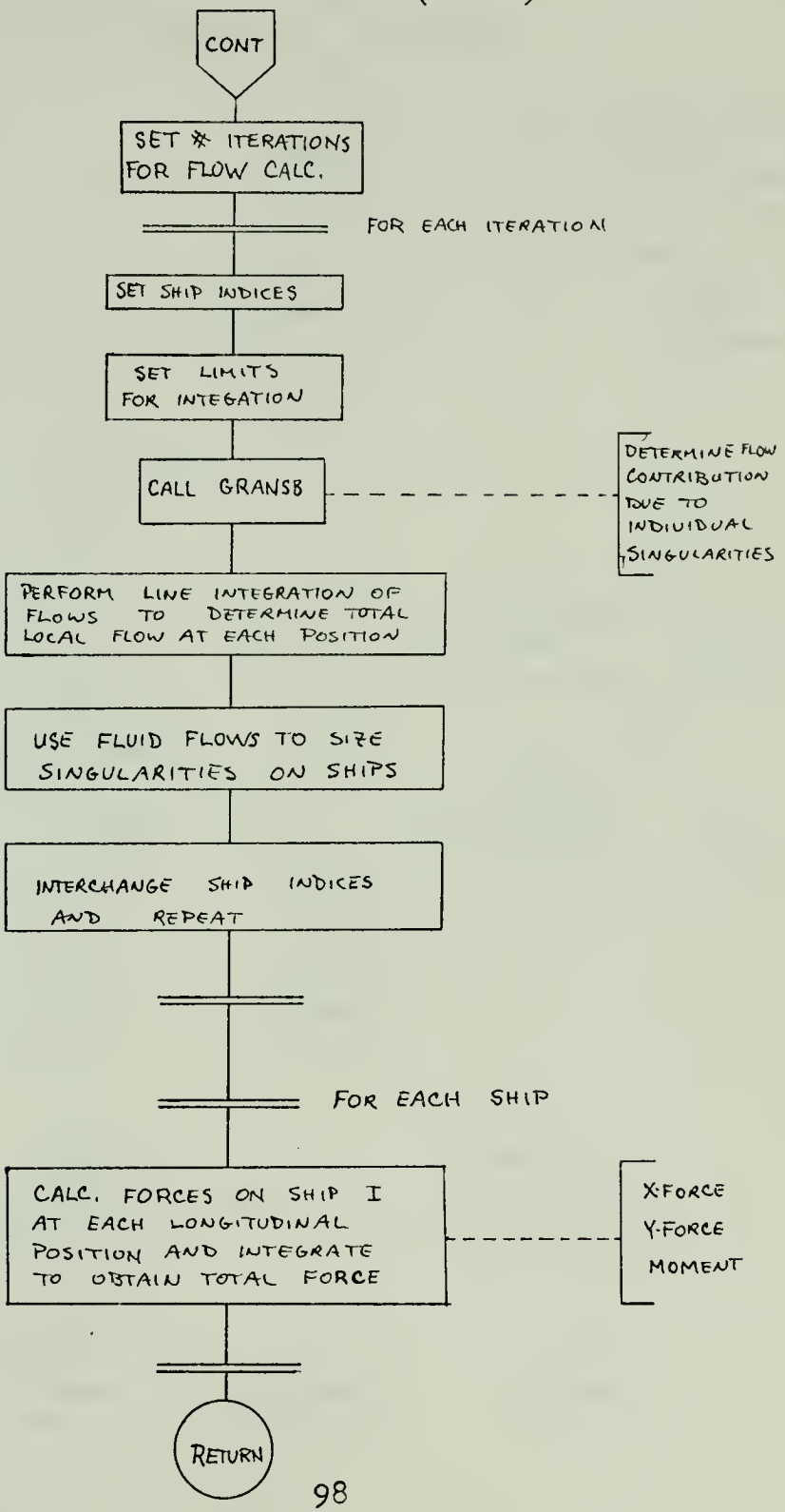

FUNCTION SIMPSN

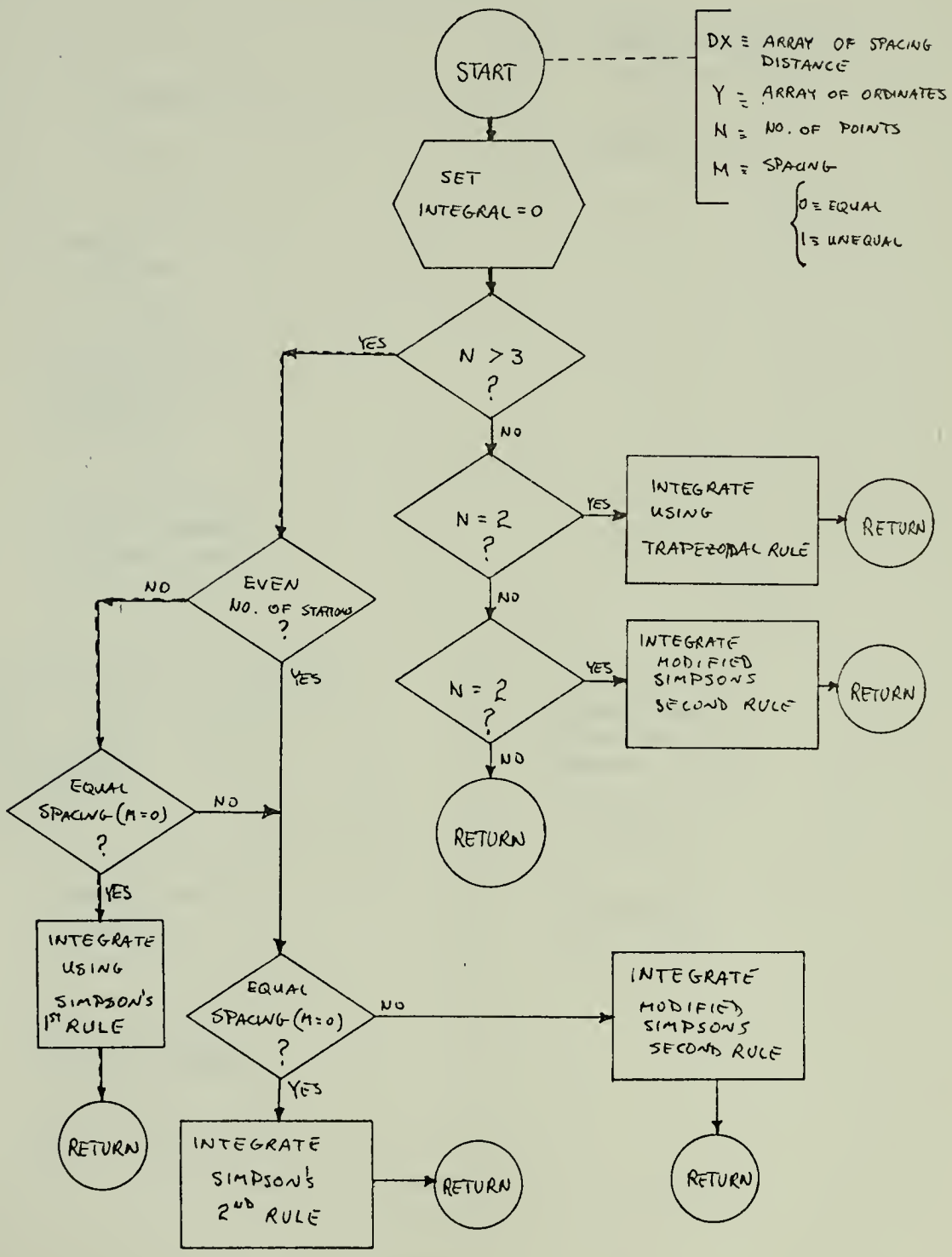

SUBROUTINE GRANSB

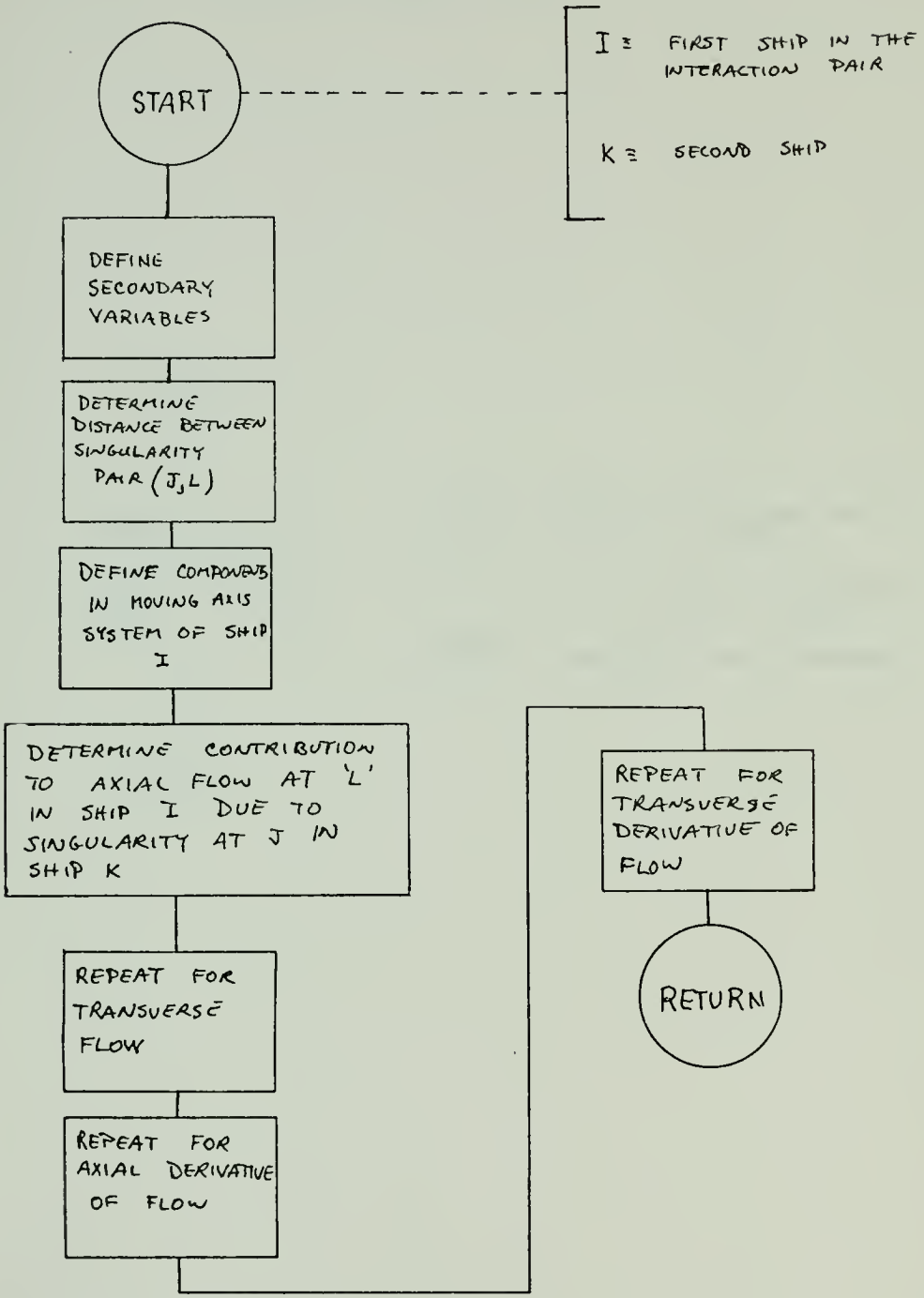

SUBROUTINE OUTPUT

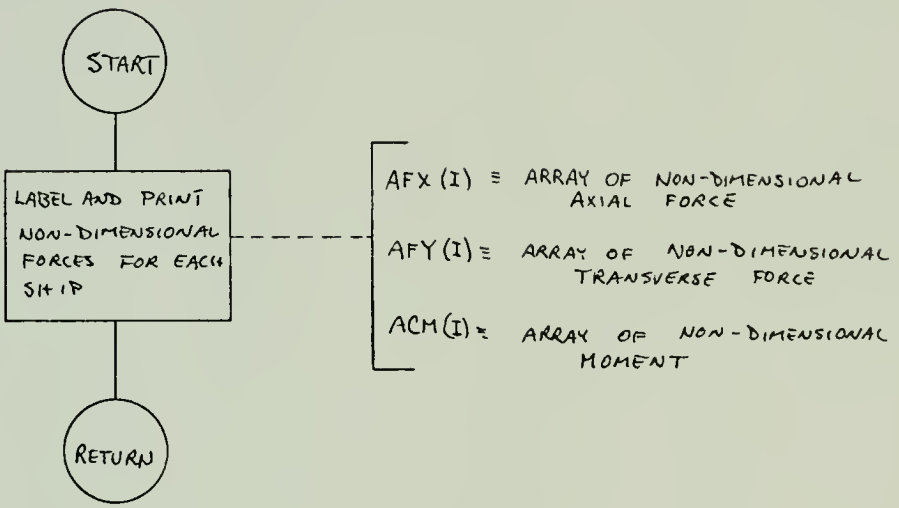

APPENDIX J

Computer Source Listing

```
C   THIS IS A PROGRAM TO CALCULATE INTERACTION FORCES                    MAINC001
C   USING A SLENDER BODY APPROXIMATION     INCLUDING END EFFECTS         MAINC002
C  MAIN PROGRAM                                                         MAIN0003
      REAL*4 LENGT                                                      MAINC004
      REAL*8 DSQRT,Z(2),R,EPS,EVAL                                      MAINC005
      INTEGER*4 N,ICV,IRITE                                             MAIN0006
      COMMON/INPUT0/SSAC(5,100),SAC(5,100),DSAC(5,100)                  MAINC007
      COMMON/INPUT1/ DISPL(5),LENGT(5),BEAM(5),VELOC(5),CP(5),CM(5)     MAINC008
      COMMON/INPUTA/ DIST(5),S(5,100),SM(5,100),SD(5,100)               MAIN0009
      COMMON/INPUTB/ NN(5),KK(5)                                        MAIN0010
      COMMON/INPUT2/ X(5),Y(5),CI(5)                                    MAINC011
      COMMON/INPUT3/ PI,ROW,M,MM,N                                      MAIN0012
      COMMON/PARAM2/ XF1(100),YF1(100),RF1(100),X1(100),Y1(100)         MAIN0013
      COMMON/PARAM3/ XF2(100),YF2(100),RF2(100),L,J                     MAINC014
      COMMON/PARAM4/ I,K                                                MAINC015
      COMMON/OUT1/ AFX(5),AFY(5),AM(5),ACM(5)                           MAIN0016
  103 PI=3.141592654                                                    MAINC017
      ROW=1.991                                                         MAINC018
      M=2                                                               MAIN0019
      MM=2                                                              MAIN0020
      L=0                                                               MAINC021
  999 CONTINUE                                                          MAIN0022
      K=2                                                               MAIN0023
      CALL INPUT                                                        MAINC024
      DO 12 I=1,N                                                       MAIN0025
      IN=NN(I)                                                          MAIN0026
      DO 10 J=1,IN                                                      MAINC027
      SAC(I,J)=SSAC(I,J)*BEAM(I)*BEAM(I)*CM(I)                          MAIN0028
   10 CONTINUE                                                          MAIN0029
      DSAC(I,1)=0.                                          delete      MAIN0030
      IP=NN(I)-1                                                        MAINC031
      DO 11 K=2,IP                                                      MAIN0032
      IA=K+1                                                            MAIN0033
      IB=K-1                                                            MAINC034
      DSAC(I,K)=(SAC(I,IA)-SAC(I,IB))/(2.*LENGT(I)/IP)                  MAIN0035
   11 CONTINUE                                                          MAIN0036
      DSAC(I,1) = DSAC(I,2)                                             ADD
      IKK = IP                                                          ADD
```

```
      IP=NN(I)                                                          MAIN0037
      DSAC(I,IP)=  DSAC(I,IKK)                                          MAIN0038
   12 CONTINUE                                                          MAIN0039
      DO 17 I=1,N                                                       MAINC040
      AFX(I)=0.                                                         MAINC041
      AFY(I)=0.                                                         MAIN0042
      AM(I)=0.                                                          MAIN0043
      SM(I,1)=1.                                                        MAINC044
   17 CONTINUE                                                          MAIN0045
      DO 40 I=1,N                                                       MAIN0046
      IA=I+1                                                            MAINC047
      IF (IA.GT.N) GO TO 31                                             MAIN0048
      DO 30 K=IA,N                                                      MAIN0049
      CALL INTSB(I,K,L)                                                 MAINC050
      AFX(K)=AFX(K)+XF2(1)                                              MAINC051
      AFY(K)=AFY(K)+YF2(1)                                              MAIN0052
      AM(K)=AM(K)+RF2(1)                                                MAINC053
      AFX(I)=AFX(I)+XF1(1)                                              MAINC054
      AFY(I)=AFY(I)+YF1(1)                                              MAIN0055
      AM(I)=AM(I)+RF1(1)                                                MAINC056
   30 CONTINUE                                                          MAIN0057
   31 CONTINUE                                                          MAIN0058
      CONST=.5*ROW*((VELOC(I)*1.6889)**2)*(LENGT(I)**2)                 MAINC059
      AFX(I)=AFX(I)/CONST                                               MAIN0060
      AFY(I)=AFY(I)/CONST                                               MAIN0061
      ACM(I)=AM(I)/(CONST*LENGT(I))                                     MAINC062
   40 CONTINUE                                                          MAINC063
      CALL OUTPUT                                                       MAIN0064
      GO TO 999                                                         MAIN0065
      END                                                               MAINC066
```

```
      SUBROUTINE INPUT                                                  INPTC001
      REAL LENGT                                                        INPTC002
      COMMON/INPUT0/SSAC(5,100),SAC(5,100),DSAC(5,100)                  INPT0003
      COMMON/INPUT1/ DISPL(5),LENGT(5),BEAM(5),VELOC(5),CP(5),CM(5)     INPT0004
      COMMON/INPUTA/ DIST(5),S(5,100),SM(5,100),SD(5,100)               INPTC005
      COMMON/INPUTB/ NN(5),KK(5)                                        INPT0006
      COMMON/INPUT2/ X(5),Y(5),CI(5)                                    INPT0007
      COMMON/INPUT3/ PI,RCW,M,MM,N                                      INPTC008
      READ (5,100,END=99) N                                             INPT0009
      DO 10 I=1,N                                                       INPT0010
      READ(5,200) DISPL(I),LENGT(I),BEAM(I),VELOC(I),CP(I),CM(I)        INPTC011
      READ(5,100) NN(I),KK(I)                                           INPTC012
      IP=NN(I)                                                          INPT0013
      READ(5,1) (SSAC(I,J),J=1,IP)                                      INPTC014
    1 FORMAT (11F5.3)                                                   INPTC015
      READ (5,200) X(I),Y(I),CI(I)                                      INPT0016
C     CONVERT DEGREES TO RADIANS                                        INPT0017
      CI(I)=PI*CI(I)/180.                                               INPTC018
   10 CONTINUE                                                          INPT0019
      WRITE (6,400) (I,LENGT(I),BEAM(I),CP(I),VELOC(I),I=1,N)           INPT0020
  400 FORMAT ('1      IDENTIFICATION OF SHIPS:',/10X,'SHIP',            INPTC021
     110X,'LENGTH',10X,'BEAM',5X,' PRISMATIC COEFFICIENT',5X,'VELOCITY',INPTC022
     2/,(9X,I3,10X,F10.3,3X,F10.3,8X,F10.3,8X,F10.3))                   INPT0023
      WRITE (6,450)                                                     INPTC024
  450 FORMAT('     SHIP POSITIONS:')                                    INPTC025
      WRITE (6,500) (I,X(I),Y(I),CI(I),I=1,N)                           INPT0026
  500 FORMAT (' SHIP',13X,'X',14X,'Y',10X,'HEADING ANGLE (RADIANS)',    INPT0027
     1/,(5X,I2,5X,F10.2,5X,F10.2,5X,F10.2))                             INPTC028
  100 FORMAT (2I5)                                                      INPT0029
  200 FORMAT (7F10.2)                                                   INPT0030
      RETURN                                                            INPTC031
   99 STOP                                                              INPTC032
      END                                                               INPT0033
```

```
      SUBRCUTINE INTSB(I,K,M)                                          ITSBC001
      REAL LENGT                                                       ITSB0002
      CCMMCN/INPUTO/SSAC(5,100),SAC(5,1CC),DSAC(5,10C)                 ITSB0003
      CCMMCN/INPUT1/ DISPL(5),LENGT(5),BEAM(5),VELOC(5),CP(5),CM(5)    ITSBCCC4
      COMMON/INPUTA/ DIST(5),S(5,1CC),SM(5,100),SD(5,1CO)              ITSBCCC5
      COMMON/INPUTB/ NN(5),KK(5)                                       ITSB0006
      CCMMCN/INPUT2/ X(5),Y(5),CI(5)                                   ITSBC007
      COMMON/INPUT3/ PI,RCW,DUMMY,MM,N                                 ITSBCCC8
      COMMON/PARAM2/ XF1(100),YF1(100),RF1(10C),X1(1CO),Y1(1CO)        ITSB0009
      CCMMCN/PARAM3/ XF2(100),YF2(100),RF2(100),L,J                    ITSBC010
      COMMON/VAR1/QR(5,100),QA(5,100),QN(5,100),DQA(5,100),DQN(5,1CO)  ITSBC011
      COMMON/VAR2/QA2(1CC),QN2(1CO),DQN2(1CO),QR2(1CO),DQA2(1CO)       ITSB0012
      CCMMCN/CUT1/ AFX(5),AFY(5),AM(5),ACM(5)                          ITSB0013
      DIMENSICN DXI(1CO),DXK(100)                                      ITSBC014
      DXI(1)=LENGT(I)/(NN(I)-1)                                        ITSB0015
      DXK(1)=LENGT(K)/(NN(I)-1)                                        ITSB0016
      N1=NN(I)                                                         ITSB0017
      N11=N1-1                                                         ITSBCC18
      N2=NN(K)                                                         ITSB0019
      N22=N2-1                                                         ITSBCC20
      XX1=LENGT(I)/2.+DXI(1)                                           ITSBC021
      YY1=LENGT(K)/2.+DXK(1)                                           ITSB0022
      IF (SM(I,1).EQ.0.) GO TO 2                                       ITSB0023
      DC 1 L=1,N1                                                      ITSBC024
      AL=L                                                             ITSB0025
      X1(L)=XX1-AL*CXI(1)                                              ITSB0026
      DXI(L)=DXI(1)                                                    ITSBC027
      S(I,L)=DSAC(I,L)*VELOC(I)*1.6889/(4.*PI)                         ITSBC028
      SM(I,L)=S(I,L)                                                   ITSB0029
      SD(I,L)=0.                                                       ITSBCC30
    1 CONTINLE                                                         ITSBC031
      S(I,1)=S(I,2)                                                    ITSB0032
      SM(I,1)=S(I,1)                                                   ITSB0033
      S(I,N1)=S(I,N11)                                                 ITSBC034
      SM(I,N1)=S(I,N1)                                                 ITSB0035
    2 CONTINUE                                                         ITSB0036
```

```
      IF(SM(K,1).EQ.0.) GO TO 4                                          ITSB0037
      DO 3 J=1,N2                                                        ITSB0038
      AJ=J                                                               ITSB0039
      Y1(J)=YY1-AJ*DXK(1)                                                ITSB0040
      DXK(J)=DXK(1)                                                      ITSB0041
      S(K,J)=DSAC(K,J)*VELOC(K)*1.6889/(4.*PI)                           ITSB0042
      SM(K,J)=S(K,J)                                                     ITSB0043
      SD(K,J)=0.                                                         ITSB0044
    3 CONTINUE                                                           ITSB0045
      S(K,1)=S(K,2)                                                      ITSB0046
      SM(K,1)=S(K,1)                                                     ITSB0047
      S(K,N2)=S(K,N22)                                                   ITSB0048
      SM(K,N2)=S(K,N2)                                                   ITSB0049
    4 CONTINUE                                                           ITSB0050
C CALCULATION OF FLOW                                                    ITSB0051
      NKK=5                                                              ITSB0052
      II=I                                                               ITSB0053
      III=K                                                              ITSB0054
      DO 30 NK=1,NKK                                                     ITSB0055
      N1=NN(II)                                                          ITSB0056
      N2=NN(III)                                                         ITSB0057
      DO 20 L=1,N1                                                       ITSB0058
      DO 10 J=1,N2                                                       ITSB0059
C CALCULATION OF FLOWS DUE TO SOURCE                                     ITSB0060
      CALL GRANSB(II,III)                                                ITSB0061
   10 CONTINUE                                                           ITSB0062
C INTEGRATE TO GET TOTAL FLOWS AT POINT ON I                             ITSB0063
      IF (II.EQ.K) GO TO 22                                              ITSB0064
      QA(I,L)=SIMPSN(DXK,QA2,N2,M)                                       ITSB0065
      QN(I,L)=SIMPSN(DXK,QN2,N2,M)                                       ITSB0066
      DQA(I,L)=SIMPSN(DXK,DQA2,N2,M)-VELOC(I)*1.6889                     ITSB0067
      DQN(I,L)=SIMPSN(DXK,DQN2,N2,M)                                     ITSB0068
C  SIZE SINGULARITIES                                                    ITSB0069
      SM(I,L)=      -QA(I,L)*DSAC(I,L)/(4.*PI)                           ITSB0070
      SD(I,L)=-2.*QN(I,L)*SAC(I,L)/(4.*PI)                               ITSB0071
      GO TO 23                                                           ITSB0072
```

```
   22 CONTINUE                                                                  ITSBC073
      QA(K,L)=SIMPSN(DXI,QA2,N1,M)                                              ITSBC074
      QN(K,L)=SIMPSN(DXI,QN2,N1,M)                                              ITSBC075
      DQA(K,L)=SIMPSN(DXI,DQA2,N1,M)- VELOC(K) * 1.6889                         ITSBC076
      DQN(K,L)=SIMPSN(DXI,DQN2,N1,M)                                            ITSBC077
C  SIZE SINGULARITIES                                                           ITSBC078
      SM(K,L)=       -QA(K,L)*DSAC(K,L)/(4.*PI)                                 ITSBC079
      SD(K,L)=-2.*QN(K,L)*SAC(K,L)/(4.*PI)                                      ITSBC080
   23 CONTINUE                                                                  ITSBC081
   20 CONTINUE                                                                  ITSBC082
      IIII=II                                                                   ITSBC083
      II=III                                                                    ITSBC084
      III=IIII                                                                  ITSBC085
      IF (II.EQ.K) GO TO 27                                                     ITSBC086
      SD(I,1)=SD(I,2)*SQRT(SAC(I,2)/PI)                                         ITSBC087
      SD(I,N1)=SD(I,N11)*SQRT(SAC(I,N11)/PI)                                    ITSBC088
      GO TO 28                                                                  ITSBC089
   27 CONTINUE                                                                  ITSBC090
      SD(K,1)=SD(K,2)*SQRT(SAC(K,2)/PI)                                         ITSBC091
      SD(K,N2)=SD(K,N22)*SQRT(SAC(K,N22)/PI)                                    ITSBC092
   28 CONTINUE                                                                  ITSBC093
   30 CONTINUE                                                                  ITSBC094
      AK=NK/2                                                                   ITSBC095
      AKK=NK                                                                    ITSBC096
      ITEST=AKK-2.*AK                                                           ITSBC097
      IF(ITEST.EQ.0) GO TO 40                                                   ITSBC098
      IIII=II                                                                   ITSBC099
      II=III                                                                    ITSBC100
      III=IIII                                                                  ITSBC101
   40 CONTINUE                                                                  ITSBC102
C     TEMP CARDS                                                               ITSBC103
      WRITE (6,200)                                                             ITSBC104
  200 FORMAT ('1',' THE FOLLOWING SINGULARITY DISTRIBUTION ARE FOR',            ITSBC105
     1' THE ELIPSOID',/,' SHIP',5X,' STATION',5X,'SOURCE STRENGTH')             ITSBC106
      WRITE (6,100) I,L,S(I)                                                    ITSBC107
  100 FORMAT (I5,5X,I5,5X,E20.10)                                               ITSBC108
```

delete

delete

```
      SD(K,L)=0.                                                        ITSB0109
      SD(I,L)=0.                                                        ITSB0110
C  END OF TEMP CARDS                                                    ITSB0111
      N1=NN(I)                                                          ITSB0112
      N2=NN(K)                                                          ITSB0113
C CALCULATION OF FORCES RPIOR TO INTEGRATION                            ITSB0114
C  CETERMINE ORCINATES FOR INTEGRATION                                  ITSB0115
      CCNST=-4.*PI*RCW/2.                                               ITSB0116
      DO 50 L=1,N1                                                      ITSB0117
      XF1(L)=CONST*(SM(I,L)*QA(I,L)-SD(I,L)*DQA(I,L))                   ITSB0118
      YF1(L)=CCNST*(SM(I,L)*QN(I,L)-SC(I,L)*DQN(I,L))                   ITSB0119
      RF1(L)=X1(L)*YF1(L)-CCNST*(QA(I,L)*SC(I,L))                       ITSB0120
   50 CONTINUE                                                          ITSB0121
C  INTERGRATE                                                           ITSB0122
      XF1(1)=SIMPSN(CXI,XF1,N1,M)                                       ITSB0123
      YF1(1)=SIMPSN(CXI,YF1,N1,M)                                       ITSB0124
      RF1(1)=SIMPSN(CXI,RF1,N1,M)                                       ITSB0125
      DC 60 J=1,N2                                                      ITSB0126
      XF2(J)=CONST*(SM(K,J)*QA(K,J)-SD(K,J)*DQA(K,J))                   ITSB0127
      YF2(J)=CONST*(SM(K,J)*QN(K,J)-SD(K,J)*DQN(K,J))                   ITSB0128
      RF2(J)=Y1(J)*YF2(J)-CCNST*(QA(K,J)*SC(K,J))                       ITSB0129
   60 CONTINUE                                                          ITSB0130
      XF2(1)=SIMPSN(CXK,XF2,N2,M)                                       ITSB0131
      YF2(1)=SIMPSN(CXK,YF2,N2,M)                                       ITSB0132
      RF2(1)=SIMPSN(CXK,RF2,N2,M)                                       ITSB0133
      RETURN                                                            ITSB0134
      END                                                               ITSB0135
```

delete

```
      FUNCTION SIMPSN(DX,Y,N,M)                                          SIMP0001
      DIMENSION DX(100),Y(100)                                           SIMP0002
      S(U,V,W,A,B,C)=A/6.*(U*(B/C+2.0)+V*(C/B+2.0)-W*A*A/B/C)            SIMP0003
      SIMPSN=0.0                                                         SIMP0004
      IF(N.GT.3) GO TO 10                                                SIMP0005
      IF(N.EQ.2) SIMPSN=0.5*DX(1)*(Y(1)+Y(2))                            SIMP0006
      IF(N.EQ.3) SIMPSN=S(Y(1),Y(2),Y(3),DX(1),DX(2),DX(1)+DX(2))        SIMP0007
     S                  +S(Y(3),Y(2),Y(1),DX(2),DX(1),DX(2)+DX(1))      SIMP0008
      RETURN                                                             SIMP0009
   10 N1=N-1                                                             SIMP0010
      IF(N-2*(N/2).NE.0.AND.M.EQ.0) GO TO 50                             SIMP0011
      IF(M.NE.0) GO TO 30                                                SIMP0012
      SIMPSN=5.*Y(1)+13.*Y(2)+7.*Y(3)-Y(4)                               SIMP0013
      DO 20 J=3,N1                                                       SIMP0014
   20 SIMPSN=SIMPSN+5.*Y(J+1)+8.*Y(J)-Y(J-1)                             SIMP0015
      SIMPSN=SIMPSN*DX(1)/12.                                            SIMP0016
      RETURN                                                             SIMP0017
   30 SIMPSN=S(Y(1),Y(2),Y(3),DX(1),DX(2),DX(1)+DX(2))                   SIMP0018
     S       +S(Y(2),Y(3),Y(4),DX(2),DX(3),DX(2)+DX(3))                  SIMP0019
      DO 40 J=3,N1                                                       SIMP0020
  110 K=J-1                                                              SIMP0021
   40 SIMPSN=SIMPSN+S(Y(J+1),Y(J),Y(K),DX(J),DX(K),DX(J)+DX(K))          SIMP0022
      RETURN                                                             SIMP0023
   50 DO 60 J=2,N1,2                                                     SIMP0024
   60 SIMPSN=SIMPSN+2.*Y(J)+Y(J+1)                                       SIMP0025
      SIMPSN=DX(1)*(Y(1)-Y(N)+2.*SIMPSN)/3.                              SIMP0026
      RETURN                                                             SIMP0027
      END                                                                SIMP0028
```

```
      SUBRCUTINE GRANSB(I,K)                                            GRSBC001
      REAL LENGT,NUM1,NUM2,NUM3                                         GRSB0002
      CCMMCN/INPUT1/ DISPL(5),LENGT(5),BEAM(5),VELOC(5),CP(5),CM(5)     GRSB0003
      CCMMCN/INPUTA/ DIST(5),S(5,100),SM(5,100),SD(5,100)               GRSBCCC4
      COMMON/INPUT2/ X(5),Y(5),CI(5)                                    GRSBCCC5
      COMMON/PARAM2/ XF1(100),YF1(1CC),RF1(1CC),X1(1C0),Y1(1CC)         GRSB0006
      CCMMCN/PARAM3/ XF2(100),YF2(100),RF2(1CC),L,J                     GRSBC007
      COMMON/VAR2/QA2(1CC),QN2(1CC),DQN2(100),QR2(100),DQA2(100)        GRSBCC08
      XX=X(K)-X(I)                                                      GRSB0009
      YY=Y(K)-Y(I)                                                      GRSBCC10
      THETA=CI(K)-CI(I)                                                 GRSBCC11
                                                                delete  [GRSB0012
      AA=XX*CCS(CI(I))+YY*SIN(CI(I))                                    GRSB0013
      BB=XX*(-SIN(CI(I)))+YY*CCS(CI(I))                                 GRSBC014
      NUM1=-AA-Y1(J)*COS(THETA)+X1(L)                                   GRSB0015
      NUM2=-BB-Y1(J)*SIN(THETA)                                         GRSB0016
      R=SQRT(NUM1*NUM1+NUM2*NUM2)                                       GRSBC017
      AX=NUM1                                                           GRSBCC18
      AY=NUM2                                                           GRSBC019
      CCNST1=AX*SIN(THETA)+AY*CCS(THETA)                                GRSBCC20
      CONST2=2.*AY*CCS(THETA)                                           GRSBCC21
      CONST3=AX*COS(THETA)+AY*SIN(THETA)                                GRSB0022
      XFCRM1=-SM(K,J)*AX/(R**3)                                         GRSB0023
      XFCRM2=-3.*SD(K,J)*AX*CONST1/(R**5)                               GRSBCC24
      XFORM3=SD(K,J)*SIN(THETA)/(R**3)                                  GRSB0025
      QA2(J)=-XFORM1-XFORM2-XFORM3                                      GRSB0026
      YFCRM1=-SM(K,J)*AY/(R**3)                                         GRSBCC27
      YFORM2=-3.*SD(K,J)*AY*CONST1/(R**5)                               GRSB0028
      YFCRM3=SD(K,J)*COS(THETA)/(R**3)                                  GRSB0029
      QN2(J)=-YFCRM1-YFCRM2-YFCRM3                                      GRSBCC3C
      XFORD1=(3.*SM(K,J)*AX*AY-3.*SD(K,J)*CCNST3)/(R**5)                GRSBC031
      XFORC2=15.*SD(K,J)*AX*AY*CONST1/(R**7)                            GRSB0032
      DQA2(J)=XFORD1+XFORC2                                             GRSBC033
      YFORD1=-SM(K,J)/(R**3)                                            GRSBC034
      YFORC2=3.*(SM(K,J)*AY*AY-SD(K,J)*(CONST1+CCNST2))/(R**5)          GRSB0035
      YFORC3=15.*SD(K,J)*AY*AY*CCNST1/(R**7)                            GRSB0036
```

```
      DQN2(J)=YFORD1+YFORD2+YFORD3                                      GRSB0037
      RETURN                                                            GRSB0038
      END                                                               GRSB0039
```

```
      SUBROUTINE OUTPUT                                                    CTPT0001
      REAL LENGT                                                           CTPT0002
      COMMON/INPUT3/ PI,RCW,M,MM,N                                         OTPTCCC3
      COMMON/OUT1/ AFX(5),AFY(5),AM(5),ACM(5)                              OTPTCCC4
      WRITE(6,400) (I,AFX(I),AFY(I),ACM(I),I=1,N)                          CTPT0005
  400 FORMAT (5X,' NON-DIMENSIONAL FORCES ON SHIP ',I2,5X,                 CTPTCCC6
     1'(MEASURED IN TERMS OF SHIPS AXIS SYSTEM)',/,5X,'AXIAL FORCE',       OTPTCCC7
     25X,'NORMAL FORCE',5X,'TOTAL MOMENT',/,5X,E10.2,5X,E10.2,5X,E10.2)    CTPT0008
      RETURN                                                               CTPTCCC9
      END                                                                  OTPTCC1C
```

Thesis
F624 Fortson
Interaction forces
between ships.